U. S. DEPARTMENT OF COMMERCE NATIONAL BUREAU OF STANDARDS

RESEARCH PAPER RP1366

Part of Journal of Research of the National Bureau of Standards, Volume 26, February 1941

INFLUENCE OF STRESS ON THE CORROSION PITTING OF ALUMINUM BRONZE AND MONEL METAL IN WATER

By Dunlap J. McAdam, Jr. and Glenn W. Geil

ABSTRACT

Cyclic stress tends to increase the size and sharpness of corrosion pits in aluminum bronze and monel metal and thus tends to increase the rate of lowering of the fatigue limit by corrosion. The form of corrosion pits in aluminum bronze is affected by the duplex microstructure. Pits in monel metal are not appreciably influenced by the microstructure. Curves of decrease of the fatigue limit, and constant-damage diagrams derived from these curves, are very different from those obtained with steels. These differences may be attributed to the fact that the rate of corrosion of aluminum bronze and monel metal, unlike that of steel, is anodically controlled. Steady stress tends to increase the rate of corrosion pitting of aluminum bronze but has little apparent effect on monel metal.

CONTENTS

I. INTRODUCTION

In a recent paper [4] [1] the authors presented results of an investigation of the influence of cyclic stress on the corrosion pitting of steels in well water. The present paper considers the influence of both cyclic and steady stresses on the corrosion pitting of aluminum bronze and monel metal.

The lowering of the fatigue limit due to stress corrosion of these nonferrous alloys has been discussed in previous papers by the senior author [1, 2].[2] At that time, however, no investigation had been made of the forms and sizes of the corrosion pits and their correlation with the cyclic stress applied during corrosion. Later, through the courtesy of the Director of the U. S. Naval Engineering Experiment Station, Annapolis, Md., the specimens that had been used were made available for such a study. This paper gives the results of this investigation and correlates the forms and sizes of the corrosion pits with the resultant lowering of the fatigue limit.

II. MATERIALS AND METHOD OF INVESTIGATION

The chemical compositions of the cold-worked aluminum bronze and monel metal are given in table 1. Aluminum bronze of this composition consists of two or more microconstituents, one of them an alpha solid solution of aluminum and iron in copper. Monel metal consists almost entirely of a single microconstituent, a solid solution. Details of the annealing treatment of these alloys for relief of internal stress are given in table 2, and tensile properties are given in table 3.

TABLE 1.—*Chemical compositions*

[Averages of two or more determinations]

Alloy	Designation	Percentages of—								
		C	Ni	Cu	Al	Fe	Mn	P	S	Si
Aluminum bronze	L-6	------	------	87.7	10.5	2.64	------	------	------	------
Monel metal	EP-8	0.16	67.5	29.5	------	1.76	0.95	0.015	0.017	0.05

TABLE 2.—*Annealing treatments for relief of internal stress*

Alloy	Designation	Temperature	Time	Cooled in—
		° *F*	*Minutes*	
Aluminum bronze	L-6	600	180	Furnace.
Monel metal	EP-8	800	180	Do.

TABLE 3.—*Tensile properties of alloys*

[Average of at least two determinations]

Alloy	Designation	Tensile strength	Johnson's limit	Proof stress (0.01%)	Elastic limit	Proportional limit	Elongation in 2 in.	Reduction of area
		lb/in.^{2}	*lb/in.*^{2}	*lb/in.*^{2}	*lb/in.*^{2}	*lb/in.*^{2}	*Percent*	*Percent*
Aluminum bronze	L-6	101,900	41,900	42,800	36,900	32,900	16.6	17.7
Monel metal	EP-8	127,200	95,000	90,000	84,500	82,000	20.6	57.8

[1] Figures in brackets indicate the literature references at the end of this paper.

[2] The aluminum bronze was previously [2] designated KF-6. In this paper it is designated L-6 to avoid confusion with the effective stress concentration factor K_F.

Each specimen used in the investigation of the forms and sizes of corrosion pits had been subjected to corrosion under a given cyclic stress and cycle frequency for a given time, and had then been dried, oiled, and subjected to fatigue test in air. The lowering of the fatigue limit was used as a measure of the damage due to the corrosion. The water used in most of the corrosion experiments was the same well water that was used in the previous experiments with steels [4]. Some of the specimens, however, had been corroded in Severn River water, a brackish water with a saline content considerably higher than that of the well water.

In studying the corrosion pits, the specimens were examined visually on the outer surface, and typical specimens were photographed. The pits were also viewed in longitudinal sections cut approximately through the axes of the specimens. To insure a correct sectional view of the pits, the polishing was done in such a way as to minimize removal of corrosion products. For this purpose, the specimens were prepared by the method of dry polishing described in the previous paper [4]. Typical micrographs were than made. The magnification required was much higher ($\times 1000$) for these micrographs than for those shown in the previous paper [4].

III. LOWERING OF THE FATIGUE LIMIT DUE TO CORROSION OF ALUMINUM BRONZE AND MONEL METAL IN FRESH WATER

1. INFLUENCE OF STRESSLESS CORROSION ON THE FATIGUE LIMIT OF ALUMINUM BRONZE AND MONEL METAL

The influence of both stressless corrosion and stress corrosion on the fatigue limit is represented by figures 1 and 2. In these figures, abscissas represent durations of corrosion and ordinates represent the fatigue limits as determined by subsequent tests without corrosion. From these diagrams are derived diagrams of several types representing the relation between stress, corrosion time, and cycle frequency for constant total and net damage. The derived diagrams will be discussed (section VI) after consideration of the results of examination of the pitted specimens.

During the stressless corrosion of steel, as shown in the previous paper [4], the fatigue limit decreases rapidly at first, but the rate of decrease gradually slackens and eventually becomes very slow. Curves representing such a variation of the fatigue limit have been termed "retarded-damage" curves. Aluminum bronze and monel metal, however, give stressless-corrosion curves of a very different type. As shown in figures 1 and 2, each of these curves is nearly horizontal at first and remains nearly horizontal throughout a long corrosion period. The slope, however, gradually increases and eventually becomes steep. Curves of this form, termed "accelerated-damage" curves, have also been obtained with stainless steel and nickel [2].

As shown in the preceding paper [4], the rate of corrosion of steel in well water is cathodically controlled (except possibly at first); that is, the rate is determined by the conditions at the cathodes. Corrosion of aluminum bronze, monel metal, stainless steel, and nickel, in well water, however, is anodically controlled; that is, the

rate of corrosion is determined by the conditions at the anodes. The evidence indicates, therefore, that cathodically controlled corrosion tends to give stressless-corrosion curves of the retarded-damage type, and that anodically controlled corrosion tends to give stressless-corrosion curves of the accelerated-damage type, such as those in figures 1 and 2. Space is not available for discussion of the types of stressless-corrosion curves obtained when the corrosion rate depends on conditions at both cathodes and anodes.

The results of corrosion generally are more erratic when the control is anodic than when it is cathodic. With anodic control, specimens corroded under apparently identical conditions may differ greatly in the resultant damage as measured by the lowering of the fatigue limit. The scatter of experimental points representing stressless corrosion, consequently, is much greater in figures 1 and 2 than in graphs representing stressless corrosion of steel in well water [4]. In an accelerating corrosion process, as in many other accelerating processes, the results are less reproducible than in a process causing retarded damage.

Stressless corrosion of aluminum bronze for more than 2 years (fig. 1) reduced the fatigue limit to less than two-thirds the original value. If the acceleration of damage should persist with increase in the corrosion time, the fatigue limit evidently would be reduced to zero in about 4 years, thus implying that corrosion pits had reached the axis of the specimen. Before this, however, the rate of lowering of the fatigue limit might begin to slacken, thus causing a reversal of the stressless-corrosion curve. (Such a delayed reversal would not affect the derived diagrams representing constant net and total damage).

Stressless corrosion of monel metal (fig. 2) would be better represented by a widening band than by a single curve. The curve as drawn takes an approximate mean course. In drawing the curve, consideration has been given not only to the experimental points representing stressless corrosion but also to the three points representing corrosion under stresses of 8,000, 10,000, and 12,000 lb/in.^{2} at 1,450 cycles per minute.

2. INFLUENCE OF STRESS CORROSION ON THE FATIGUE LIMIT OF ALUMINUM BRONZE AND MONEL METAL

The stress-corrosion curves for aluminum bronze and monel metal, unlike many of the curves for steels [4], descend at an increasing rate. The scatter of experimental points generally is greater for a stress-corrosion curve than for a stressless-corrosion curve. The scatter is much greater for monel metal than for aluminum bronze. Even though several experiments were made with monel metal at a number of the stresses, the scatter of results is so great that the curves could not be accurately established. Some experiments caused fatigue failure during corrosion, whereas other experiments at the same stress and for about the same corrosion time caused little damage. Such results indicate that an ideal stress-corrosion curve would show an accelerated increase of slope and final abrupt drop to zero ordinate. The curves are so drawn in figures 1 and 2. Each curve is drawn so as to follow an approximate mean course.

Under simultaneous corrosion and cyclic stress, the lowering of the fatigue limit evidently is more rapid than under stressless corrosion.

For a given cycle frequency, the rapidity of descent of a curve increases with the cyclic stress; for a given stress, the rapidity of descent increases with the cycle frequency. Even at very low cycle frequencies (ranging from 5 cycles per hour to 1 cycle per day), however, sufficiently high stress and sufficiently long duration of corrosion may cause much net damage (figs. 1 and 2). The quantitative relation between stress, cycle frequency, corrosion time, and either net or total damage [3] is discussed in section VI.

IV. PITS CAUSED BY CORROSION OF ALUMINUM BRONZE WITH AND WITHOUT STRESS

1. INFLUENCE OF THE MICROSTRUCTURE ON THE CORROSION PITTING OF ALUMINUM BRONZE

The position and form of corrosion pits in steels, in aerated well water, are little affected by the microstructure [4]. The pits are free to assume the forms determined by the corrosion conditions. Pitting in the aluminum bronze used in these experiments, however, was much influenced by the microstructure. This is illustrated by the positions and forms of the pits caused by corrosion of a specimen in salt water. The water used for this purpose was Severn River water, which generally has about one-sixth the saline content of sea water. The specimen was corroded under stress of 60,000 lb/in.^{2} at 1 cycle per day for 16 days. Surface views are shown in figure 9 and longitudinal sections are shown in figure 10.

Views *A* and *B* of figure 9 show the surface of this corroded specimen after slight polishing with magnesium oxide. The polishing was merely enough to remove most of the corrosion products from the cathodic areas and reveal the pits. The dark areas, shown in view *A* at 100 magnification and in view *B* at 500 magnification, are pits filled with corrosion products. These corroded areas are in the delta phase of the alloy. The nearly white, uncorroded areas are in the alpha solid solution. The alpha phase evidently is cathodic to the delta phase and to the associated iron-rich constituent.

After considerable additional polishing with magnesium oxide, the surface appears as shown in views *C* and *D*. The cathodic areas are now practically free from corrosion products, and the dendritic structure of the alloy is clearly revealed. The corrosion pits in this alloy generally are not free to assume the roughly hemispherical or saucer-like forms that are found after corrosion of steels [4]. The pits in the aluminum bronze are bounded by the frondlike crystallites of the cathodic alpha phase.

This influence of the microstructure is revealed not only by the surface views but also by the sectional views (fig. 10). Whereas pits in steel tend to deepen perpendicularly to the surface, the pits in the aluminum bronze follow the interstices between adjacent crystallites of the alpha solid solution. Many of the pits thus take an oblique direction (fig. 10). This influence of the microstructure is found not only after corrosion in salt water but also after the much slower corrosion in fresh water. Numerous instances of this influence will be found in the micrographs now to be considered.

[3] Total damage due to stress-corrosion is measured by the vertical distance of a stress-corrosion curve (at any point) below the origin of the curve. Net damage is the difference between the total damage and the damage that would be caused in the same time by stressless corrosion.

Although the entire delta phase tends to be anodic during corrosion in either salt water or well water, pitting in well water is not continuous throughout the delta constituent. Some parts of this phase evidently are more anodic than others. Very little information about the forms and distribution of the corrosion pits, therefore, can be obtained by examining the darkened anodic areas on the surface. In this investigation, consequently, attention has been confined almost entirely to longitudinal sections. Results of the investigation are shown in figures 11 to 26, inclusive.

2. PITS CAUSED BY STRESSLESS CORROSION OF ALUMINUM BRONZE IN WELL WATER

Although results of stressless corrosion of five specimens of aluminum bronze in well water are shown in figure 1, only four of these specimens were available for examination of the corrosion pits. Sectional views of these specimens are shown in figures 11 and 12.

Corrosion for 66 days (view *A*, fig. 11) has caused numerous small pits. The forms of most of these pits evidently have been influenced greatly by the duplex microstructure of the alloy. A few of the pits are roughly hemispherical, like pits caused by stressless corrosion of steel. After corrosion for 88 days, the pits shown in view *B* of figure 11 are smaller than those shown in view *A*. The lowering of the fatigue limit, however, was slightly greater after corrosion for 88 days than after corrosion for 66 days (fig. 1). The sections shown in figure 11, *B*, therefore, probably do not traverse the regions of deepest pitting on this specimen. As the variation of pitting in a specimen generally is greater when the process is anodically controlled than when it is cathodically controlled, sectional views of the most deeply pitted regions can be obtained less easily with aluminum bronze (and monel metal) than with steels.

After corrosion for much longer than 66 days (fig. 12), the pits have increased greatly in size, and the influence of microstructure on the forms of the pits evidently has become less prominent. Although most of the pits here shown have the saucerlike form found after long corrosion of steels, some of the pits show the confining influence of the alpha phase. The lowering of the fatigue limit (fig. 1) was much greater after corrosion for 640 and 1,021 days than after 66 and 88 days. This must be attributed largely to the influence of corrosion time on the size of the pits. The slightness of the effect of the pits shown in figure 11 evidently is due to their small size [4].

After corrosion of steel in well water for only 4 and 4.7 days (figs. 9 and 33 of the previous paper [4]),[4] the pits were much larger and the lowering of the fatigue limit was much greater than after corrosion of aluminum bronze in well water for 66 and 88 days (fig. 11).

Values of the effective stress concentration factor, K_F, obtained by stressless corrosion of steels,aluminum bronze, and monel metal are assembled in table 4. The values for the breadth and depth of pits have been taken from the sectional views of the pits that probably would cause the highest values of K_F. These were obtained from figures 9, 10, and 33 of the first paper and figures 11, 12, 22, 23, and 24 of the present paper. The values of K_F were obtained from the corresponding diagrams, one of which is not found in either of these two papers.[5]

[4] In such comparison, allowance must be made for the fact that the magnification of the sectional views in this paper is 4 to 20 times as great as the magnifications used in the previous paper.

[5] The diagram for steel AX–W–10 is in a previous paper [3] by the senior author.

TABLE 4.—*Sizes of stressless-corrosion pits and corresponding values of the effective stress-concentration factor, K_F*

Metal	Designation	Water	Days	Size of pit		Ratio 5:6	K_F
				Breadth	Depth		
1	2	3	4	5	6	7	8
				Inches	*Inches*		
Steel	AX-W-10	Well	2	0.0024	0.0014	1.71	1.09
Do	AX-W-10	do	4.7	.006	.0024	2.5	1.35
Do	IW-W-10	do	10	.010	.003	3.3	1.47
Do	AX-W-10	do	47	.012	.007	1.71	1.61
Do	IW-W-10	do	50	.013	.005	2.6	1.71
Do	IW-W-10	do	100	.025	.011	2.27	1.83
Aluminum bronze	L-6	do	66	.004	.002	2.0	1.05
Do	L-6	do	640	.00055	.0004	1.37	1.54
Do	L-6	do	1,021	.00065	.0004	1.62	1.76
Monel metal	EP-8	do	122	.0008	.0004	2.0	1.10
Do	EP-8	do	157	.0009	.00045	2.1	1.10
Do	EP-8	do	170	.0011	.0009	1.22	1.20
Do	EP-8	do	170	.0005	.0011	0.45	1.20

For the steels, the value of K_F evidently tends to increase with increase in the breadth of the corrosion pits. A similar relationship is found for aluminum bronze and monel metal in well water. If table 4 were arranged solely in the order of increasing breadth of the corrosion pits, however, this would not be the order of increasing value of K_F. The values obtained with aluminum bronze in well water for 640 and 1,021 days are too high to be in the order of increasing breadth of corrosion pits. (Some of the values for monel metal also are too high for such an arrangement.)

By plotting values of the breadth of a pit as abscissas and corresponding values of K_F-1 as ordinates, the points obtained with steels in well water would give a curve starting from the origin of coordinates and rising at a decreasing rate. (Such a curve is also obtained by fatigue tests with specimens having notches of the same form but differing in size.) The points obtained with aluminum bronze in well water for 640 and 1,021 days would be above this curve. Probable reasons for this are found by considering the ratios of breadth to depth of the pits. For the steels in well water, the mean value of this ratio is about 2.3; that is, the pits generally are roughly hemispherical. For the aluminum bronze, after corrosion for 640 and 1,021 days, the ratio is only about 1.5. The relatively high values of K_F obtained with these specimens, therefore, may be attributed in part to the fact that the relative depth of the pits is greater in this alloy than in steels. They may be attributed in part, however, to the angularity of some of the corrosion pits, the angularity resulting from the duplex microstructure of the aluminum bronze. The differences in the values of K_F in table 4 evidently are due not only to differences in size but also to differences in the forms of the pits.

3. PITS CAUSED BY STRESS CORROSION AT 1,450 CYCLES PER MINUTE

In studying the influence of cyclic stress on the forms and sizes of corrosion pits, the pits caused by stressless corrosion will be compared with the pits caused by simultaneous corrosion and cyclic stress. Attention will be given first to specimens that have been subjected

to various stresses with a frequency of 1,450 cycles per minute. Typical sectional views are shown in figure 13. These were obtained after corrosion for short times.

The forms of nearly all these pits have been greatly influenced by the duplex microstructure. The pits, therefore, are similar in form to many of the pits caused by stressless corrosion (figs. 11 and 12). The cyclic stress, however, evidently has had much influence on the size of the pits. After corrosion at 30,000 lb/in.^{2} for only 1.8 days, the pits (view *A*) are nearly as large as those found after stressless corrosion for 66 days (fig. 11, *A*). After corrosion at 25,000 lb/in.^{2} for 6 days (fig. 13, *B*), the pits are nearly as large as those found after stressless corrosion for 640 days (fig. 12, *A*). After corrosion at 20,000 lb/in.^{2} for 11 days (fig. 13, *C*), some of the pits are larger than those found after stressless corrosion for 1,021 days (fig. 12, *B*). Moreover, the ratio of depth to breadth, for some of the pits shown in figure 13, is greater than for the pits found after stressless corrosion. Although no distinct fissures or crevices (such as those found after corrosion of steels at this cycle frequency) are found in figure 13, the cyclic stress probably has increased the sharpness of the salients in this alloy. Cyclic stress evidently influences the size and form of the corrosion pits in aluminum bronze as well as in steels.

To facilitate comparison between the corrosion pits and the corresponding lowering of the fatigue limit, three different symbols are used for the experimental points in figures 1 and 2. A triangle is used when the sectional view gives distinct evidence of fissures; a square is used when no fissures are visible; a circle is used when the pits have not been examined.

The pits in any specimen tend to vary more widely when the corrosion process is anodically controlled than when it is cathodically controlled. Correlation between a sectional view of corrosion pits and the lowering of the fatigue limit, therefore, is less satisfactory for aluminum bronze than for steels. If the pits shown in figure 13 were the most advanced pits in these three specimens, these views would be in the order of increasing damage. Actually, however, they are in the order of decreasing damage (fig. 1). The pit at which fatigue fracture started probably was more advanced than any of the pits found in a sectional view. The resultant damage evidently depended on the increased size and sharpness of a few of the most advanced pits, not visible in figure 13.

The apparent absence of damage (fig. 1) due to the pits shown in figure 13 (*C*) may be attributed to a locally high fatigue limit for this specimen. The pits shown in figure 13 (*C*), although they appear large at this high magnification, are smaller than pits caused by stressless corrosion of steel for a much shorter time in well water (fig. 9 of the preceding paper [4]).

4. PITS CAUSED BY STRESS CORROSION AT 10,000 CYCLES PER MINUTE

Corrosion with a cycle frequency of 10,000 per minute at 30,000 lb/in.^{2} for 0.3 day has caused the pits shown in view *A* of figure 14. One of the pits here shown is about as large as any of those found after stressless corrosion for 66 days (fig. 11, *A*). The pits shown in figure 14 (*A*), moreover, generally have greater relative depth than those found after stressless corrosion. Some of the pits, especially

those extending in oblique direction, are very sharp. From one of these a crack has started. A crack such as this evidently caused the fatigue failure during the corrosion stage (fig. 1).

5. PITS CAUSED BY STRESS CORROSION AT 500 CYCLES PER MINUTE

Corrosion with a cycle frequency of 500 per minute has caused the pits shown in views *B*, *C*, and *D* of figure 14. After corrosion at 60,000 lb/in.^{2} for 0.06 day (view *B*), some pits are nearly as large as those found after corrosion for 640 days without stress (fig. 12, *A*). The cyclic stress, moreover, evidently has caused the sharp projections generally extending in an oblique direction. To sharp salients such as these may be attributed the rapid decrease of the fatigue limit during corrosion (fig. 1). As this specimen did not fail by fatigue during corrosion, the cracks starting from some of the sharp salients (fig. 14, *B*) may have started during the subsequent fatigue test.

The sharp projections extending inward from the corrosion pits shown in views *A* and *B* of figure 14 probably are crevices and fissures[6] similar to those caused by stress corrosion of steels. In aluminum bronze, however, the crevices and fissures generally are not free to advance in a plane perpendicular to the axis of the specimen, as they do in steels. The planes of extension, both inward and along the surface of the specimen, are determined largely by the direction of the crystallites of the alpha phase. All these fissures probably have started at blunt pits and have extended both inward and along the surface. A sectional view, in aluminum bronze as in steel [4], however, may not traverse the origin of a fissure.

Corrosion at 40,000 lb/in.^{2} for 0.7 day has caused the pits shown in figure 14 (*C*). As the corrosion caused considerable damage (fig. 1), this damage must be attributed to larger or sharper pits than those revealed in figure 13 (*C*). A similar discrepancy exists between the damage and the pits shown in figure 13 (*D*).

6. PITS CAUSED BY STRESS CORROSION AT 50 CYCLES PER MINUTE

Corrosion with a cycle frequency of 50 per minute has caused the pits shown in figure 15. After corrosion at 50,000 lb/in.^{2} for 1.1 days (view *A*), some pits are nearly as large as those found after stressless corrosion for 640 days (fig. 12, *A*). The cyclic stress, moreover, has caused sharp oblique projections, as shown in some of the sections. To such projections, which probably are sections of fissures, may be attributed the rapid lowering of the fatigue limit (fig. 1). These fissures probably started at blunt pits, such as those shown in figure 15 (*A*), and extended both along the surface and inward.

After corrosion at 35,000 lb/in.^{2} for 6.7 days (fig. 15, *B*), some of the pits are larger than those found after stressless corrosion for 1,021 days (fig. 12, *B*). One of the pits shown in figure 15 (*B*) has extended inward in an oblique direction and has incipient sharp projections. To such projections and to the increased size of the pits may be attributed the lowering of the fatigue limit, as shown in figure 1.

After corrosion at 20,000 lb/in.^{2} for 52 days, the pits are larger than those found after stressless corrosion for 66 days (fig. 11, *A*). Because

[6] Crevices, as defined in the previous paper [4], are merely fissures that have not advanced far enough to be visible on the surface of the specimen at low magnification. No attempt will be made in this paper to distinguish between crevices and fissures.

of the small size of these pits (only about 0.0005-inch diameter), their effect on the fatigue limit was inappreciable (fig. 1).

7. PITS CAUSED BY STRESS CORROSION AT 10 CYCLES PER MINUTE

Corrosion with a cycle frequency of 10 per minute has caused the pits shown in figure 16. After corrosion at 40,000 lb/in.^{2} for 13 days (view *A*), some pits are as large as those found after stressless corrosion for 1,021 days (fig. 12, *B*). Sharp projections extend obliquely inward. The largest of these pits is the origin of sharp projections, which probably are sections of fissures. This view, unlike those in figures 14 (*A*) and (*B*) and 15 (*A*), shows the blunt pit from which the fissures started. The fissures have caused considerable damage (fig. 1).

After corrosion at 30,000 lb/in.^{2} for 26 days (fig. 15, *B*), the pits are about as large as those found after stressless corrosion for 66 days (fig. 11, *A*). Incipient sharp projections, such as those here shown, may account for the considerable decrease in the fatigue limit (fig. 1).

8. PITS CAUSED BY STRESS CORROSION AT 0.5 CYCLE PER MINUTE

Corrosion with a cycle frequency of 0.5 per minute has caused the pits shown in figure 17. After corrosion at 60,000 lb/in.^{2} for 6 days, the pits found in view *A* are very small; one of the blunt pits, however, is relatively deep. A few sharp pits extending inward from the surface probably are sections of fissures which started at blunt pits not shown in this view. This effect of the cyclic stress accounts for the considerable damage shown in figure 1.

After corrosion at 50,000 lb/in.^{2} for 13 days (fig. 18, *B*), some of the pits are as large as those found after stressless corrosion for 640 days (fig. 12, *B*). Sharp pits, moreover, extend obliquely inward from the surface. The blunt origins of these sharp pits are not traversed by this section. The lowering of the fatigue limit of this specimen was not as great as would be expected.

9. PITS CAUSED BY STRESS CORROSION AT 5 CYCLES PER HOUR

Corrosion with a cycle frequency of 5 per hour has caused the pits shown in figures 18 and 19. After corrosion at 60,000 lb/in.^{2} for 15 days (fig. 18, *A*), the pits are as large as those found after stressless corrosion for 1,021 days (fig. 12, *B*). One of the sections, moreover, shows an oblique pit, which probably is an incipient fissure. The increased size and sharpness of the pits, due to the cyclic stress, account for the lowering of the fatigue limit (fig. 1).

After corrosion at 50,000 lb./in.^{2} for 24 days (fig. 18, *B*), the pits are considerably larger than those found after stressless corrosion for 1,021 days. Nevertheless, the pits are much smaller than those caused by corrosion of steel in well water for 10 days (fig. 9, *D* of the first paper [4]). The sharp oblique projections from one of the pits in figure 18 (*B*) probably are incipient fissures. The lowering of the fatigue limit was about the same for this specimen as for the specimen represented in figure 18 (*A*).

After corrosion at 30,000 lb/in.^{2} for 339 days, the pits shown in figure 19 are only about as large as those found after stressless corrosion for 66 days (fig. 11, *A*). This specimen, therefore, probably contained much larger pits than those traversed by the section.

Numerous sharp projections, however, extend inward from pits and from the surface of the specimen. To these sharp fissures may be attributed the great decrease of the fatigue limit (fig. 1).

10. PITS CAUSED BY STRESS CORROSION AT 1 CYCLE PER HOUR

Corrosion with a cycle frequency of 1 per hour has caused the pits shown in figure 20. After corrosion at 60,000 lb/in.^{2} for 20 days (view *A*), the pits are larger than those found after stressless corrosion for 66 days (fig. 11, *A*) but no fissures are visible. The effect on the fatigue limit, as shown in figure 1, was small. About the same effects on the pits and on the fatigue limit were caused by corrosion at 40,000 lb/in.^{2} for 73 days (fig. 20, *B*). Corrosion at the same stress for a much longer time (fig. 20, *C*), however, caused sharp projections, which probably are sections of fissures. The development of these fissures has caused rapid descent of the curve of decrease of the fatigue limit (fig. 1).

After corrosion at 35,000 lb/in.^{2} for 374 days (fig. 20, *D*), no large pits are found. This specimen, however, probably contained much larger pits than those traversed by the sectional view. Sharp fissures extend obliquely inward from the surface and from some of the small pits. To the sharp fissures must be attributed the great decrease in the fatigue limit (fig. 1). (In a few more days, this specimen probably would have failed during corrosion.)

11. PITS CAUSED BY STRESS CORROSION AT 1 CYCLE PER DAY

Corrosion with 1 cycle per day has caused the pits shown in figure 21. After corrosion at 60,000 lb/in.^{2} for 28 days (view *A*), the pits are nearly as large as those found after stressless corrosion for 640 days (fig. 12, *A*). The pits have lowered the fatigue limit slightly. After corrosion at 40,000 lb/in.^{2} for 151 days, sharp projections are found (view *B*, fig. 21). In some regions, these sharp salients are intermingled with portions of the alpha phase. Pits of the same type, moreover, are found after corrosion at the same stress for 240 days (view *C*). The sharp salients, together with interspersed portions of the alpha phase, form pits larger than those found after stressless corrosion for 1,021 days (fig. 12, *B*). The great effect of such pits on the fatigue limit is illustrated by the descent of the curve in figure 1.

V. PITS CAUSED BY CORROSION OF MONEL METAL WITH AND WITHOUT STRESS

1. PITS CAUSED BY STRESSLESS CORROSION OF MONEL METAL IN WELL WATER

The distribution of corrosion pits on the specimens of monel metal was far from uniform. The pits generally were found in clusters. Through such a cluster in each specimen a section was cut and polished for microscopic examination. After the pits in this section were photographed, the section generally was polished again so as to remove about 0.001 inch of metal. The removal of this thin layer of metal generally revealed other corrosion pits. In this manner, photographs of several sections sometimes were obtained. In assembling the photographs of each specimen, no attempt was made to distinguish between the different sections.

Only a few of the many specimens of monel metal that were subjected to corrosion were available for examination of the corrosion pits. The pits were examined in only three of the nine specimens (fig. 2) that had been subjected to stressless corrosion. Sectional views of these three specimens are shown in figures 22, 23, and 24.

After stressless corrosion for 122 days (fig. 22), the pits are small. Although some pits appear large at this high magnification, they are much smaller than the pits caused by corrosion of steel for only a few days (fig. 9 of the previous paper [4]). As monel metal is essentially a single-phase alloy, the pits are little influenced by the microstructure. The pits shown in figure 22, consequently, are roughly hemispherical or saucerlike, resembling in this respect the pits caused by brief corrosion of steel. Because of their bluntness and small size, these pits have had little effect on the fatigue limit (fig. 2).

After stressless corrosion for 157 days (fig. 23), some of the pits are broader, but no deeper, than after corrosion for 122 days. Some of the pits resemble in form and size the pits shown in figure 22. The fatigue limit of this specimen, moreover, was about the same as that of the specimen corroded for 122 days.

Larger pits were found after stressless corrosion for 170 days (fig. 24). Sharp projections, moreover, have formed on some of the pits; other sharp pits have extended inward from the surface. As these sharp pits were formed without stress, they probably are rootlike projections rather than transverse fissures. Rootlike pits may be formed in either steels or nonferrous metals under the influence of concentration gradients of oxygen or of an anion or cation. The fatigue limit of this specimen was lower than that of all the other stressless-corrosion specimens of this alloy, even specimens that had been corroded for much longer times. Typical stressless-corrosion pits in monel metal, therefore, probably resemble in form those seen in figures 22 and 23 rather than those seen in figure 24. This conclusion is supported by results of examination of pits caused by stress corrosion.

2. PITS CAUSED BY STRESS CORROSION OF MONEL METAL AT 1,450 CYCLES PER MINUTE

Corrosion with a cycle frequency of 1,450 per minute has caused the pits shown in figure 25. After corrosion at 30,000 lb/in.^{2} for 10 days, only a few very small pits are visible even at this high magnification (view *A*). They probably are not much larger than if the specimen had been corroded without stress. Rounded pits of this size (about 0.0001-inch diameter) have practically no effect on the fatigue limit [4]. The fatigue limit, however, was not much more than half that of an uncorroded specimen (fig. 2). Some pits in this specimen, therefore, probably were much larger or sharper than if the specimen had been corroded without stress. This is one of the few experiments (at high frequency) that were stopped in the midst of the nearly vertical descent of the stress-corrosion curve. As this steep descent probably was due to the rapid development of a single fatigue crack from one of the corrosion pits, the chance of finding the rounded pit from which the crack started was very small.

After corrosion at 10,000 lb/in.^{2} for 331 days (fig. 25, *B*) some of the pits are much larger than those caused by stressless corrosion for 170 days (fig. 24). Most of this difference in size probably is due to the cyclic stress. The great decrease of the fatigue limit caused by

stress corrosion of this specimen (fig. 2), however, probably should be attributed to the development of a crevice, fissure, or fatigue crack from a sharp projection, such as the one pointing inward from the largest pit in figure 25. As shown in the previous paper [4], the effective stress-concentration factor increases with both the size and the sharpness of the pits.

3. PITS CAUSED BY STRESS CORROSION OF MONEL METAL AT 5 CYCLES PER HOUR

Corrosion with a cycle frequency of 5 per hour has caused the pits shown in figure 26. After corrosion at 45,000 lb/in.^{2} for 123 days (view *A*), the pits are larger than those found after stressless corrosion for about the same time (fig. 22), and are about as large as those found after stressless corrosion for 170 days (fig. 24). Some of the pits in figure 26 (*A*), moreover, have small sharp projections, which probably represent incipient fissures. The effect of the cyclic stress on the size and form of the pits, however, was not great enough to cause much net damage (fig. 2). Corrosion for a little longer time probably would have caused rapid development of transverse fissures and rapid descent of the corresponding curve in figure 2.

Corrosion at 40,000 lb/in.^{2} for 148 days has caused the pits shown in view *B* of figure 26. Although the corrosion time was longer for this specimen than for the specimen represented in view *A*, the moderate increase in time would not be expected to compensate for the decrease in stress. As would be expected, therefore, the pits shown in view *B* appear less damaging than those shown in view *A*. Although some of the pits shown in view *B* are broader than those in view *A*, they are shallower and show no evidence of incipient fissures. The pits evidently have caused very little net damage (fig. 2).

VI. NET AND TOTAL DAMAGE DUE TO STRESS CORROSION OF ALUMINUM BRONZE AND MONEL METAL IN WELL WATER

1. TYPES OF DIAGRAMS REPRESENTING NET AND TOTAL DAMAGE

From figures 1 and 2, other diagrams have been derived to represent the interrelation between stress, corrosion time, cycle frequency, and total number of cycles, for constant net and total damage. These diagrams are shown in figures 3 to 8. Diagrams of the types shown in figures 3, 4, and 5 are shown in previous papers by the senior author [1, 2]. Since that time, however, stress-corrosion experiments with aluminum bronze were continued so as to remove all uncertainty as to the forms of these diagrams.[7] The additional information thus made available, together with the information obtained by examination of the corrosion pits, leads to definite conclusions as to the process of stress corrosion of these alloys.

2. DIAGRAMS REPRESENTING CONSTANT NET DAMAGE

The diagrams in figures 3, 4, and 5 represent the relation between stress, corrosion time, cycle frequency, and total number of cycles, for 15 percent net damage. This amount of net damage is represented

[7] These experiments were made with the cooperation of W. C. Stewart, Metallurgist of the U. S. Naval Engineering Experiment Station, with the permission of the Director of the Station.

by the broken line below each stressless corrosion line in figure 1. Each of these broken lines is drawn so that the ordinate at any point is 85 percent of the corresponding ordinate of the stressless-corrosion line. The intersections of the broken lines with the stress-corrosion lines are used in deriving the diagrams in figures 3, 4, and 5.

In figures 3 and 4, the diagrams may be considered to represent plan views of three-dimensional diagrams, in which the "vertical" coordinates (perpendicular to the plane of figs. 3 and 4) represent stresses in the corrosion stage. The curves in figures 3 and 4 thus represent contour lines on the surface of the three-dimensional diagrams. Complementary views of the three-dimensional diagrams for these two alloys are shown in figure 5. Each diagram in this figure represents lines on the surface as viewed in the direction of the arrow in figures 3 and 4. Diagrams *A* and *C* of figure 5 represent views of constant-frequency lines, which are seen in figures 3 and 4 as straight diagonal lines. Diagrams *B* and *D* of figure 5 show lines representing constant numbers of cycles, which are seen as constant-ordinate lines in figures 3 and 4. Diagrams of this type have not been considered in previous papers.

The form of the diagram for aluminum bronze (fig. 3) is well established by means of the experimental points. The curves as drawn, however, are not based only on the positions of these experimental points. The curves in this diagram and in the complementary diagrams (*A* and *B* of fig. 5) are so drawn that the three diagrams represent correlated views of a three-dimensional diagram. The diagram in figure 3 has thus been extended to lower stresses and cycle frequencies than those used in actual experiments. The extrapolated portion of the diagram may be considered qualitatively correct.

The form of the corresponding diagram for monel metal (fig. 4) also is well established by means of the experimental points. The diagram for monel metal evidently is qualitatively similar to the diagram for aluminum bronze. Drawn in accordance with the evidence and in proper correlation with the complementary diagrams (*C* and *D*, fig. 5), the diagram in figure 4 may be considered qualitatively correct.

The diagrams in figures 3 and 4 are very different from the corresponding diagram obtained with steels in well water, figure 6, of the previous paper [4]. Whereas all the curves in that diagram, as they extend to the right, approach a horizontal direction, all the curves in figures 3 and 4 approach a vertical direction. This difference in form is due chiefly to the difference in form of the curves representing stressless corrosion. When the stressless-corrosion curve is of the retarded-damage type, the derived diagram tends to be of the form obtained with steels in well water. When the stressless-corrosion curve is of the accelerated-damage type (figs. 1 and 2), the derived diagram tends to be of the form shown in figures 3 and 4.[8] The great difference in form of these diagrams representing constant net damage, therefore, may be attributed to the difference in the type of control of the rate of corrosion. Anodic control tends to give a diagram of the form shown in figures 3 and 4.

All the diagrams in figure 5 are similar in form. The lines representing low frequencies (in diagrams *A* and *C*) and the lines representing small numbers of cycles (in diagrams *B* and *D*) are nearly straight,

[8] The diagrams representing constant net damage thus resemble qualitatively the diagrams representing constant total damage, figures 6 and 7.

as are all the lines in the corresponding diagrams for steels in well water [4]. With increase in the cycle frequency or in the total number of cycles, however, the curvature of the lines increases and the slope decreases.

From the slope of a low-frequency line, an estimate can be made of the influence of stress on the rate of net damage. As shown in the preceding paper [4], the linear logarithmic relationship may be represented by the equation $R=CS^n$, in which R represents the mean rate of net damage, S the stress, and C and n are constants. The exponent n is the cotangent of the angle of slope of the line. As indicated by the slopes of the lines representing 1 cycle per day in figure 5, the value of n (for this cycle frequency) is 3.5 for aluminum bronze and about 2.1 for monel metal. The rate of net damage evidently varies as a power of the stress. As represented by the curved lines in figure 5, however, the power exponent increases with the stress and with the cycle frequency. In this respect, the diagrams for aluminum bronze and monel metal differ from the corresponding diagram for steels (fig. 5 of the preceding paper [4]).

3. DIAGRAMS REPRESENTING CONSTANT TOTAL DAMAGE

A diagram to represent constant total damage may be derived from families of curves of the type shown in figures 1 and 2 by utilizing the coordinates of intersections of such curves with a given horizontal line. An index of the total damage corresponding to this horizontal line is the effective stress concentration factor, K_F, obtained by dividing the fatigue limit of an uncorroded specimen by the fatigue limit of the corroded specimen [4].

Two-dimensional diagrams representing constant total damage may be of several types, representing different views of a three-dimensional diagram. In figures 6, 7, and 8 are diagrams of three types, corresponding to the three types of diagrams representing constant net damage (figs. 3, 4, and 5). The diagrams in figures 6 and 7 are plan views of three-dimensional diagrams for aluminum bronze and monel metal, respectively. In figure 8, the diagrams represent views in the direction of the arrows in figures 6 and 7. In diagrams A and C of figure 8, the lines are constant-frequency lines; in diagrams B and D, each line represents the indicated total number of cycles. The total damage on which each diagram is based is indicated by the value of K_F. At the right of each of the diagrams in figures 6 and 7 and at the left of each diagram in figure 8, is a straight boundary line which represents the time necessary to reach the indicated value of K_F through stressless corrosion. The course of each curve represents the influence of cycle frequency (or number of cycles) in shortening the time necessary to cause constant total damage.

In the plan diagram for aluminum bronze (fig. 6), each curve approaches a vertical direction. The curves, however, do not approach the same vertical asymptote. With the possible exception of curves representing stresses less than about 25,000 lb/in.^{2}, none of the curves approaches the time boundary of the diagram, the line representing stressless corrosion. A diagram of this form evidently indicates that the influence of stress on corrosion would be about the same for all cycle frequencies less than about 1 cycle per day. The evidence in figure 6 thus implies that the corrosion pitting of aluminum bronze is accelerated by steady stress. The relation between steady stress

and time for constant net damage evidently is represented approximately by the curve representing 1 cycle in figure 8 (*B*).

The plan diagram for monel metal (fig. 7) is qualitatively similar to the diagram for aluminum bronze. The diagram for monel metal, however, has not been extended to sufficiently low cycle frequencies to determine whether or not all the curves approach the time boundary of the diagram. If they do, steady stress (at least up to 80,000 lb/in.^{2}) has no appreciable effect on the corrosion pitting of this alloy. Comparison of figures 6 and 7, however, shows conclusively that the influence of steady stress is much less for monel metal than for aluminum bronze. The same conclusion would be reached by comparing the diagrams for these two alloys in figure 8.

Diagrams representing constant total damage for steels in fresh water (not shown) differ greatly from the diagram for aluminum bronze (fig. 6). In a plan diagram for steels, all the curves approach the time boundary, thus indicating that steady stress (at least up to the maximum value used in the investigation) has no appreciable effect on the corrosion pitting of steel in fresh water. As shown in the preceding paper [4], an influence of steady stress on corrosion would not be expected when the rate of corrosion is cathodically controlled, but is possible when the rate is anodically controlled.

VII. THE PROCESS OF STRESS CORROSION OF ALUMINUM BRONZE AND MONEL METAL IN AERATED FRESH WATER

The evidence presented in previous sections indicates that cyclic stress tends to increase the size and sharpness of corrosion pits in aluminum bronze and monel metal. The effect tends to increase with the stress and with the cycle frequency. The effect of stress on the corrosion pitting of these two alloys thus resembles qualitatively the effect of stress on the corrosion pitting of steels. For steels in well water [4], however, the accelerating influence of cyclic stress is caused chiefly by an increase in the permeability of the coating of corrosion products. Cyclic stress increases the permeability in both cathodic and anodic regions and tends to shift the process from a cathodically controlled toward an anodically controlled process. An increase in the stress or the cycle frequency thus opposes the tendency of the process to shift, with time, toward purely cathodic control. As the corrosion of aluminum bronze and monel metal is an anodically controlled process, the rate of corrosion pitting depends not only on the initial stress but also on the enhanced stress due to stress concentration around the corrosion pits. The rate of pitting thus tends to be accelerated. As with any accelerating process, the results are less reproducible than the results obtained by stress corrosion of steels in well water [4].

The accelerating influence of steady stress on the corrosion pitting of aluminum bronze may be due to an increase in the solution pressure, especially in the regions of high stress concentration around corrosion pits. This influence of stress is superposed on the influence of an increased permeability of the anodic coating owing to the cyclic stress.

The difference in behavior of monel metal and aluminum bronze under steady stress may be caused, at least in part, by the fact that aluminum bronze has a duplex microstructure, whereas monel metal

is a single-phase alloy. The difference, however, may be caused in part by the greater strength of the monel metal and in part by a difference in the permeabilities of the anodic coatings. The influence of stress on the solution pressure would be important only when the stress is locally high enough to cause plastic deformation and when the anodic coating is so permeable that the permeability is not the controlling factor.

As will be shown in a later paper, however, steady stress accelerates the corrosion pitting of steel in distilled water, even when the nominal stress is far below any index of elastic strength. An influence of steady stress on corrosion evidently is favored by conditions causing a slow corrosion rate, with anodic control. Such conditions, when the stress is high enough, tend to cause sharp, deep corrosion pits, which increase the local stress and thus accelerate the advance of the pit.

VIII. SUMMARY

Corrosion pits in the aluminum bronze, unlike the pits in steels, generally are not free to assume a roughly hemispherical form but are confined between crystallites of the alpha phase. Pits in monel metal are more like those in steel. Pits in aluminum bronze and monel metal are much smaller than those in steel. Cyclic stress tends to increase both the size and sharpness of the pits. The effective stress concentration that causes the lowering of the fatigue limit depends on both the size and the sharpness [4]. A sufficiently high combination of stress, cycle frequency, and corrosion time causes fissures to develop from blunt pits. Fissures in the aluminum bronze generally are oblique, whereas fissures in steel and monel metal tend to be perpendicular to the direction of the principal tensile stress.

The curves of decrease of the fatigue limit with corrosion time are of the accelerated-damage type. Such curves are obtained when the corrosion rate is anodically controlled. With these two alloys, therefore, the pits in a specimen have a wider range of size and sharpness than the pits formed under cathodic control, as in steels. The pit that caused the lowering of the fatigue limit may have been much larger and sharper than the pits found in the sectional views. The damage may then be greater than the sectional views would indicate. Many of the sectional views, however, give good correlation with the resultant fatigue limits.

Steady stress tends to accelerate corrosion of aluminum bronze but has little apparent effect on the corrosion pitting of monel metal.

Acknowledgement is made to H. O. Willier for the development of the method of polishing and for the careful preparation and photographing of the metal specimens.

IX. REFERENCES

[1] D. J. McAdam, Jr., *Stress and corrosion*, Report Proc. Third International Congress of Applied Mechanics, Stockholm, **2** 269–293 (1930).

[2] D. J. McAdam, Jr., *Influence of stress on corrosion*, Trans. Am. Inst. Min. Met. Engrs., Inst. of Metals Div. **99**, 282–318 (1932).

[3] D. J. McAdam, Jr., *Stress corrosion of metals*, Proc. Zurich Congress, Int. Assn. Testing Materials **1**, 228–246 (1931).

[4] D. J. McAdam, Jr., and G. W. Geil, *Influence of cyclic stress on the corrosion pitting of steels in fresh water, and the influence of stress corrosion on the fatigue limit*, J. Research NBS **24**, 685 (1940) RP1307.

WASHINGTON, November 29, 1940.

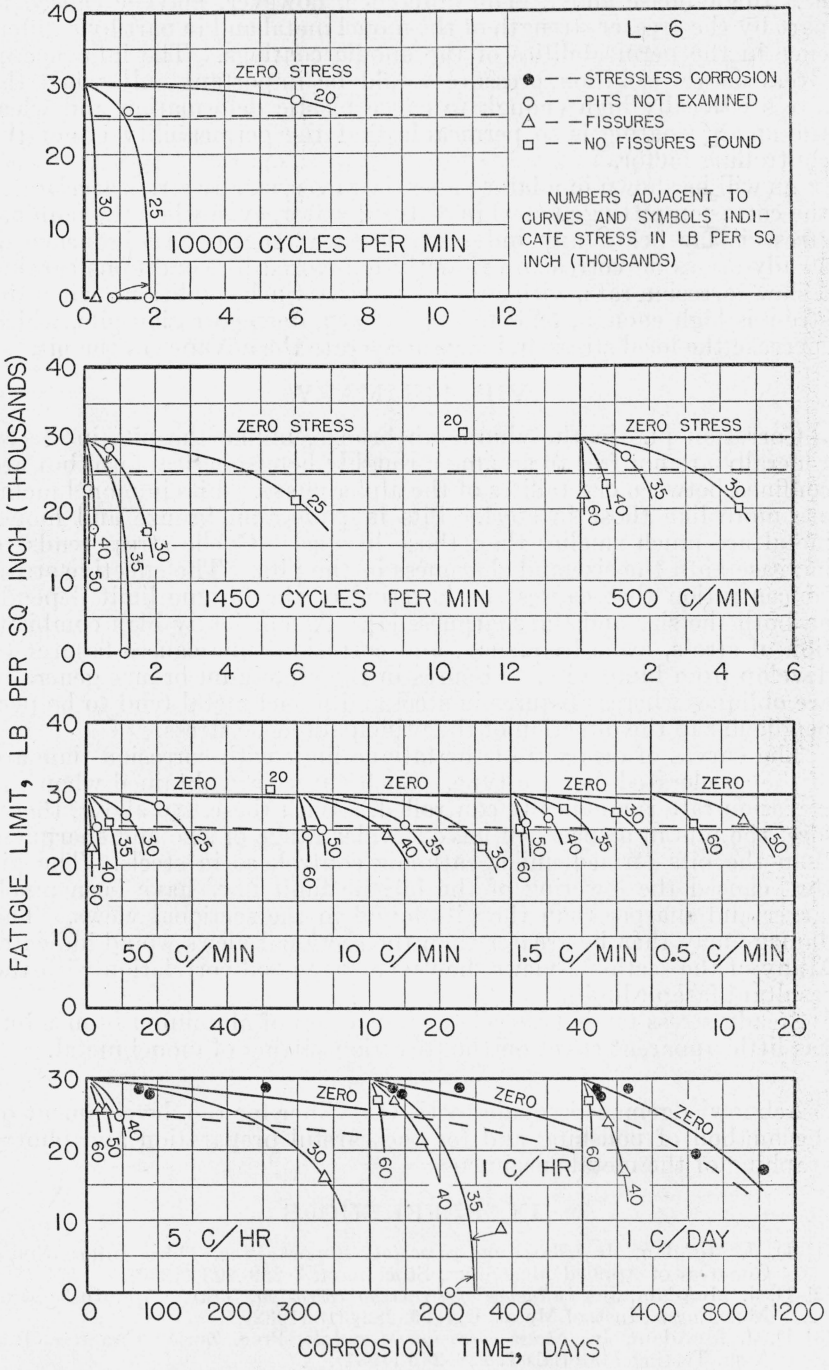

FIGURE 1.—*Influence of corrosion, with and without stress, on the fatigue limit of aluminum bronze.*

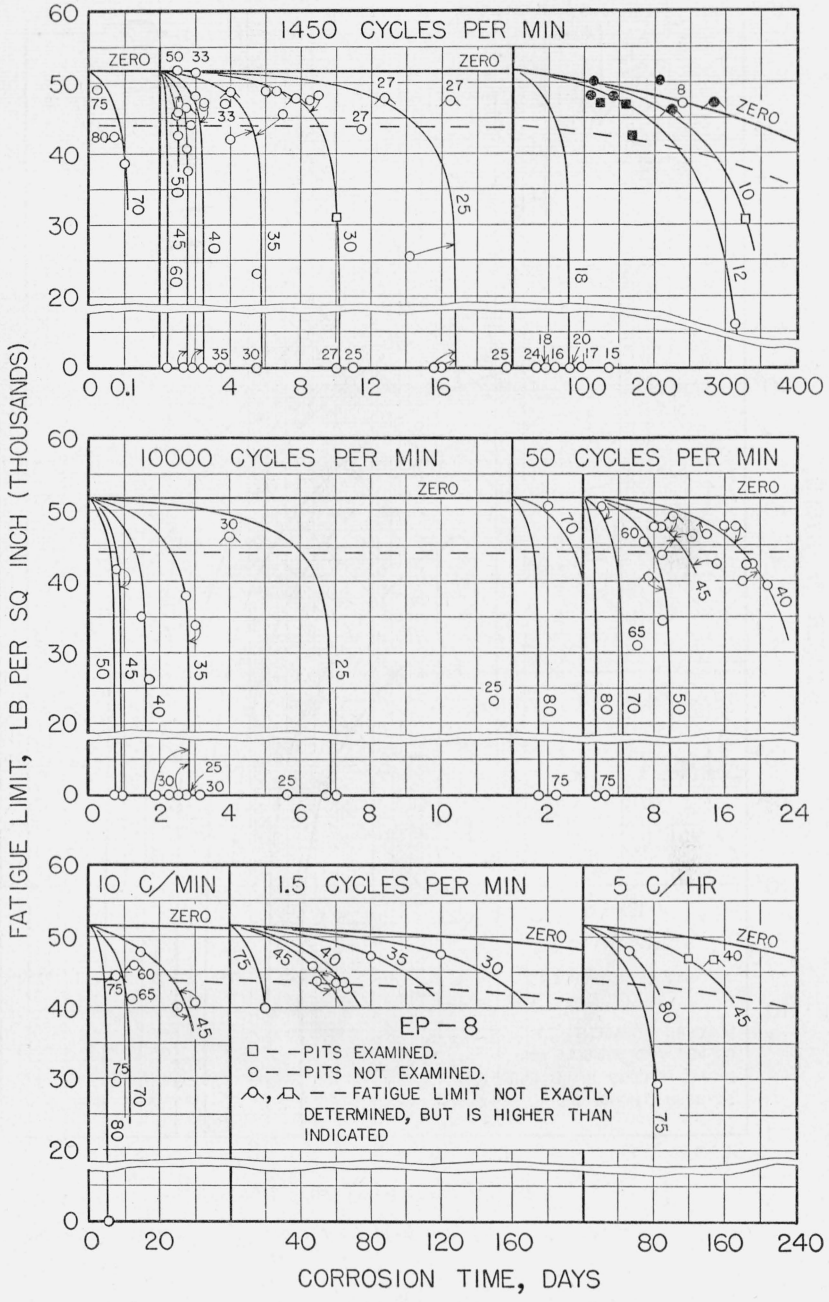

FIGURE 2.—*Influence of corrosion, with and without stress, on the fatigue limit of monel metal.*

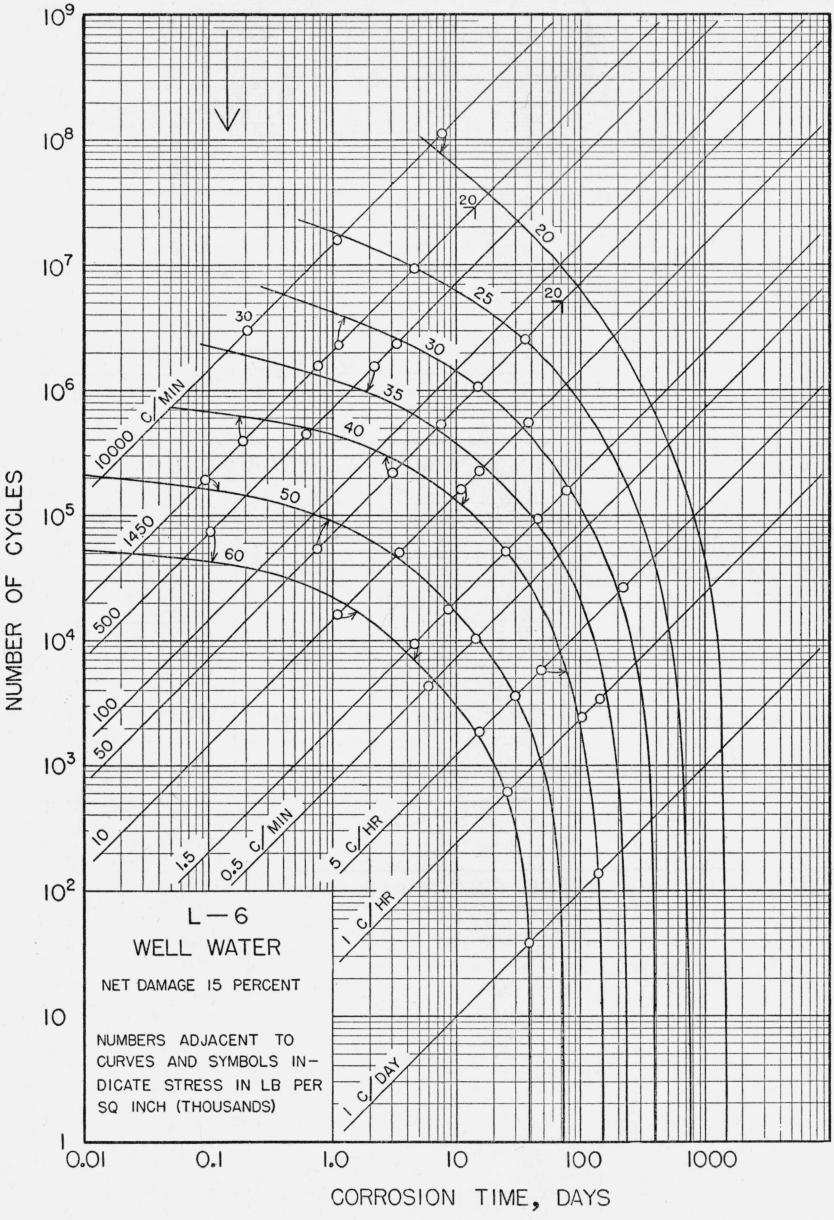

FIGURE 3.—*Constant net damage due to stress corrosion of aluminum bronze.*

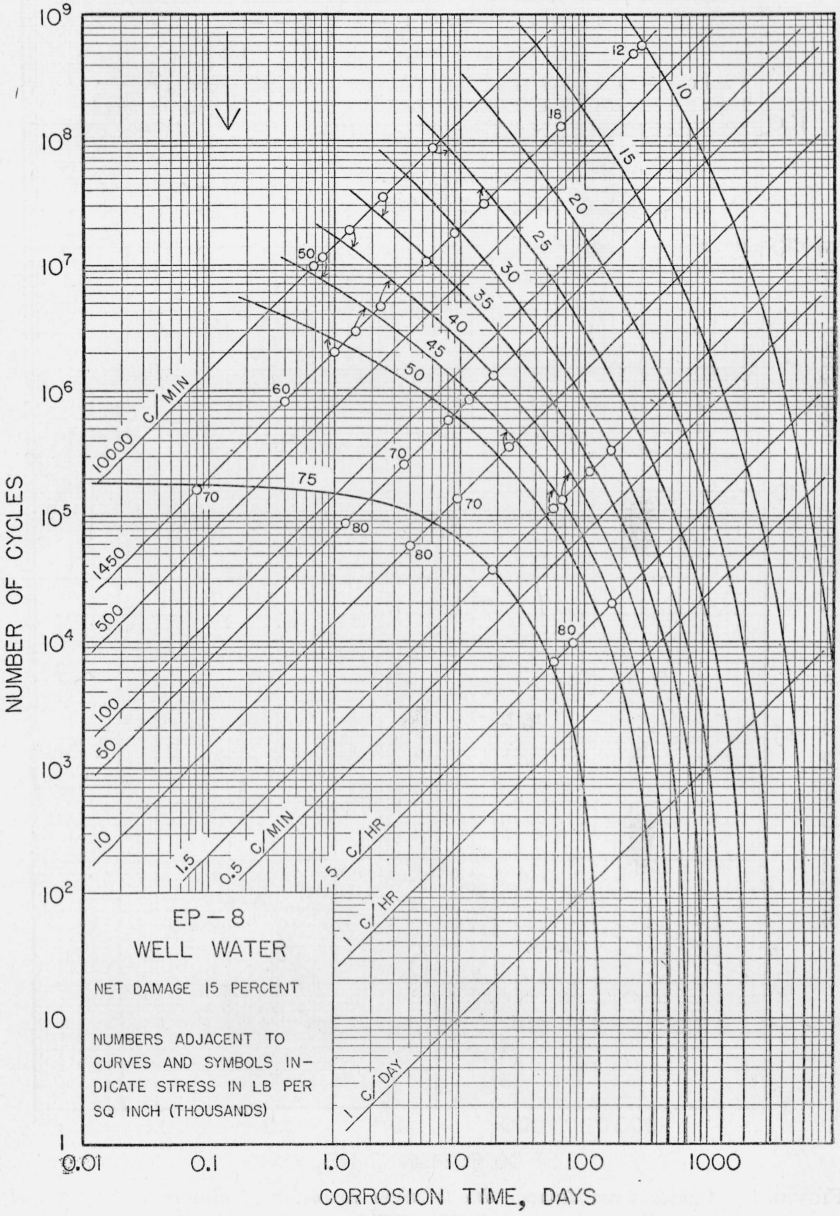

FIGURE 4.—*Constant net damage due to stress corrosion of monel metal.*

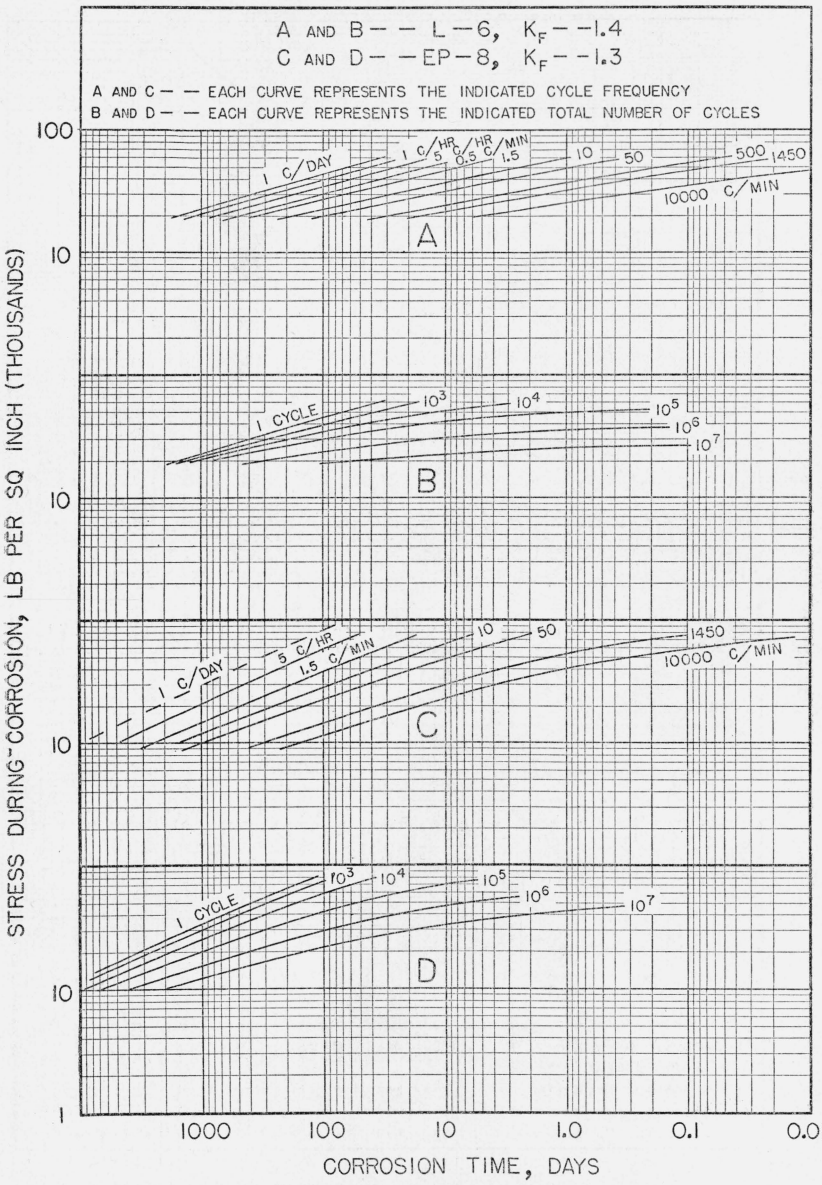

FIGURE 5.—*Constant net damage due to stress corrosion of aluminum bronze and monel metal.*

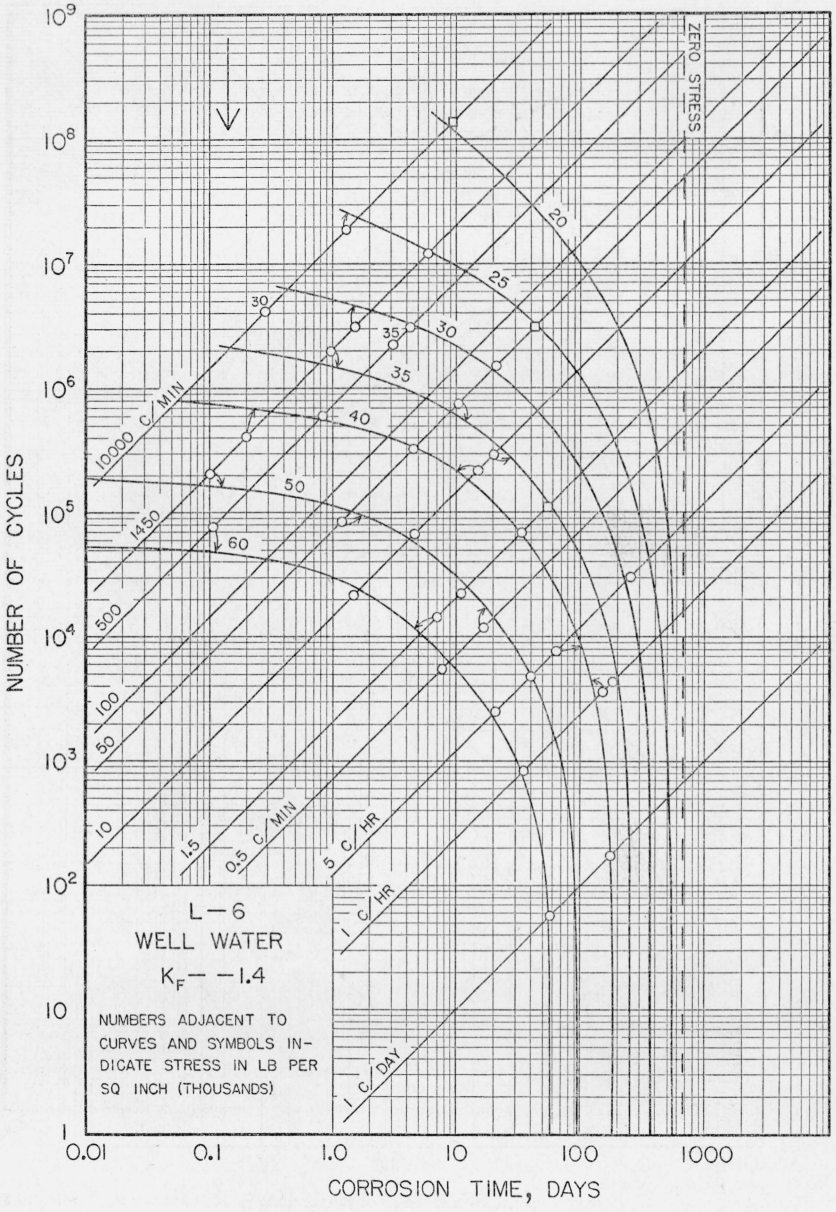

FIGURE 6.—*Constant total damage due to stress corrosion of aluminum bronze.*

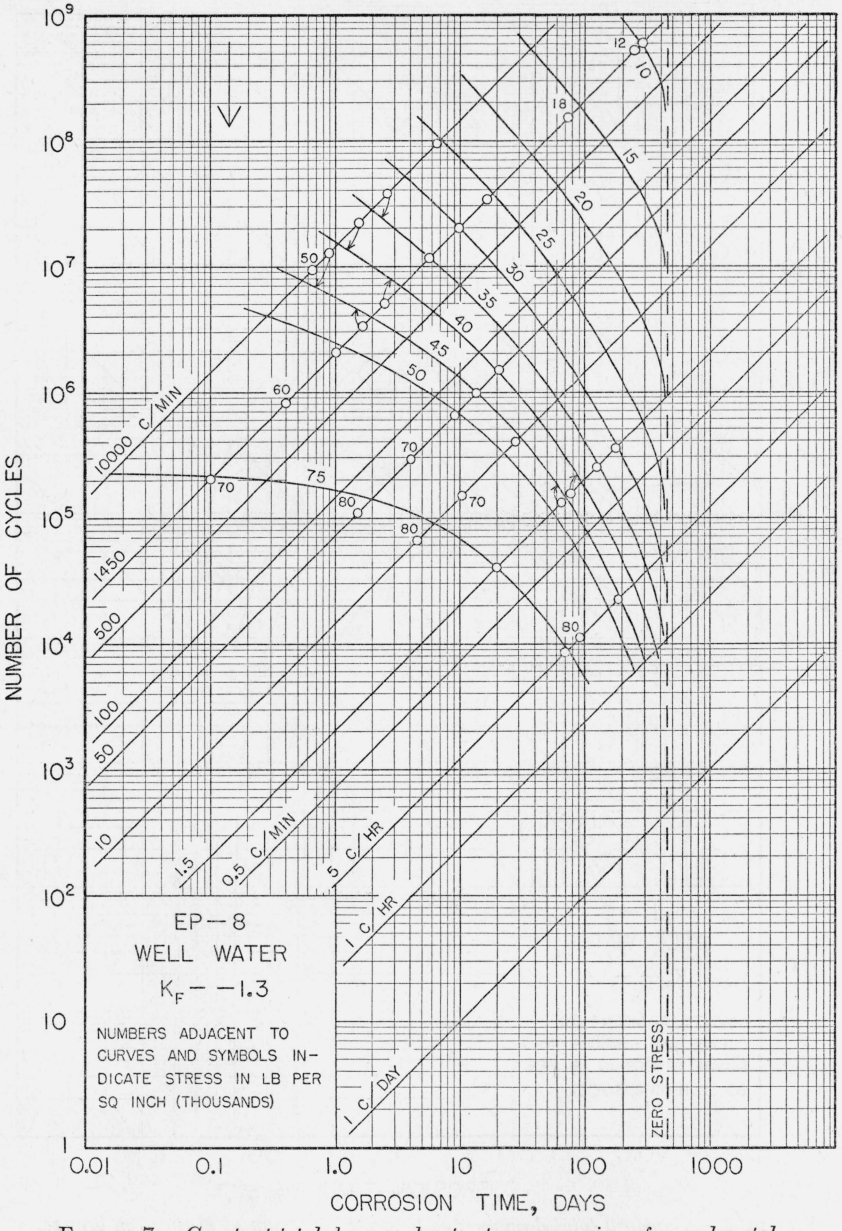

FIGURE 7.—*Constant total damage due to stress corrosion of monel metal.*

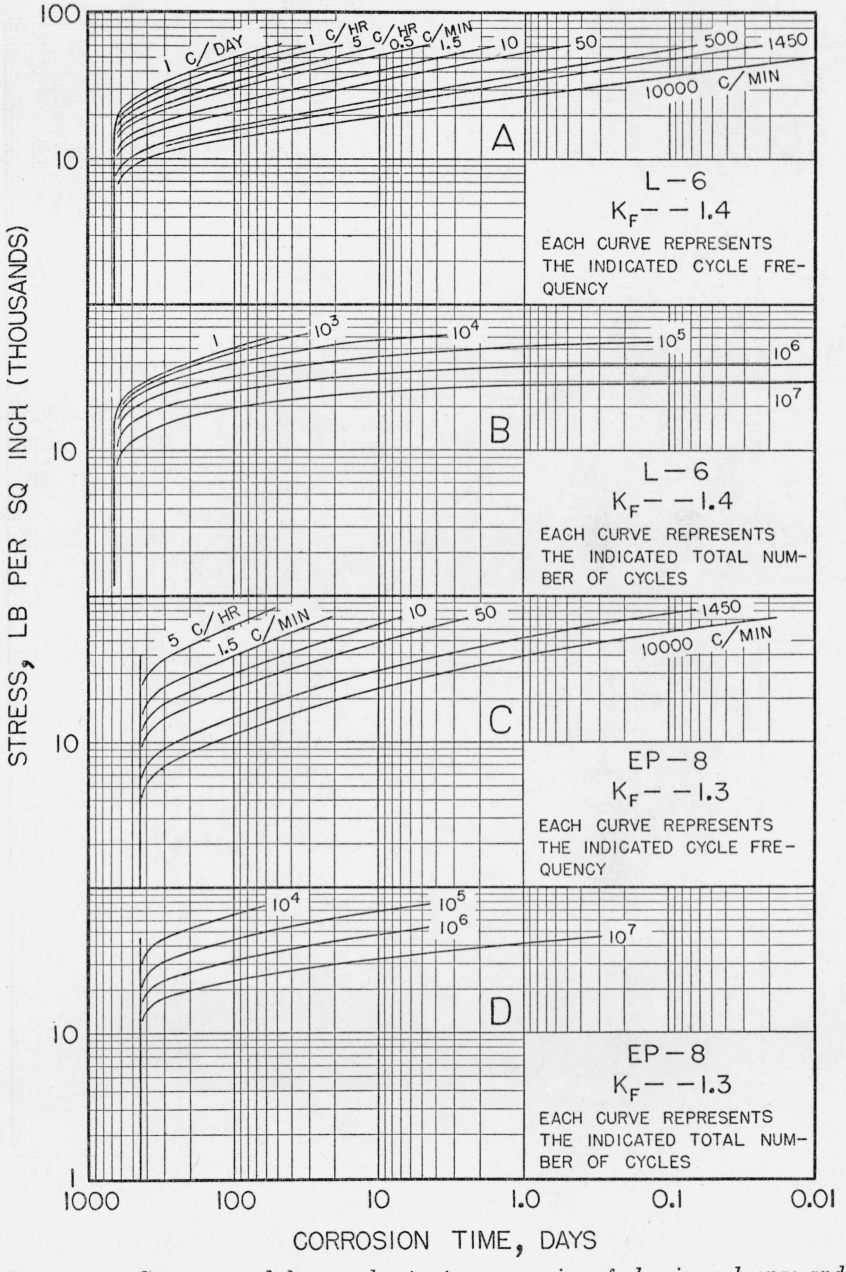

FIGURE 8.—*Constant total damage due to stress corrosion of aluminum bronze and monel metal.*

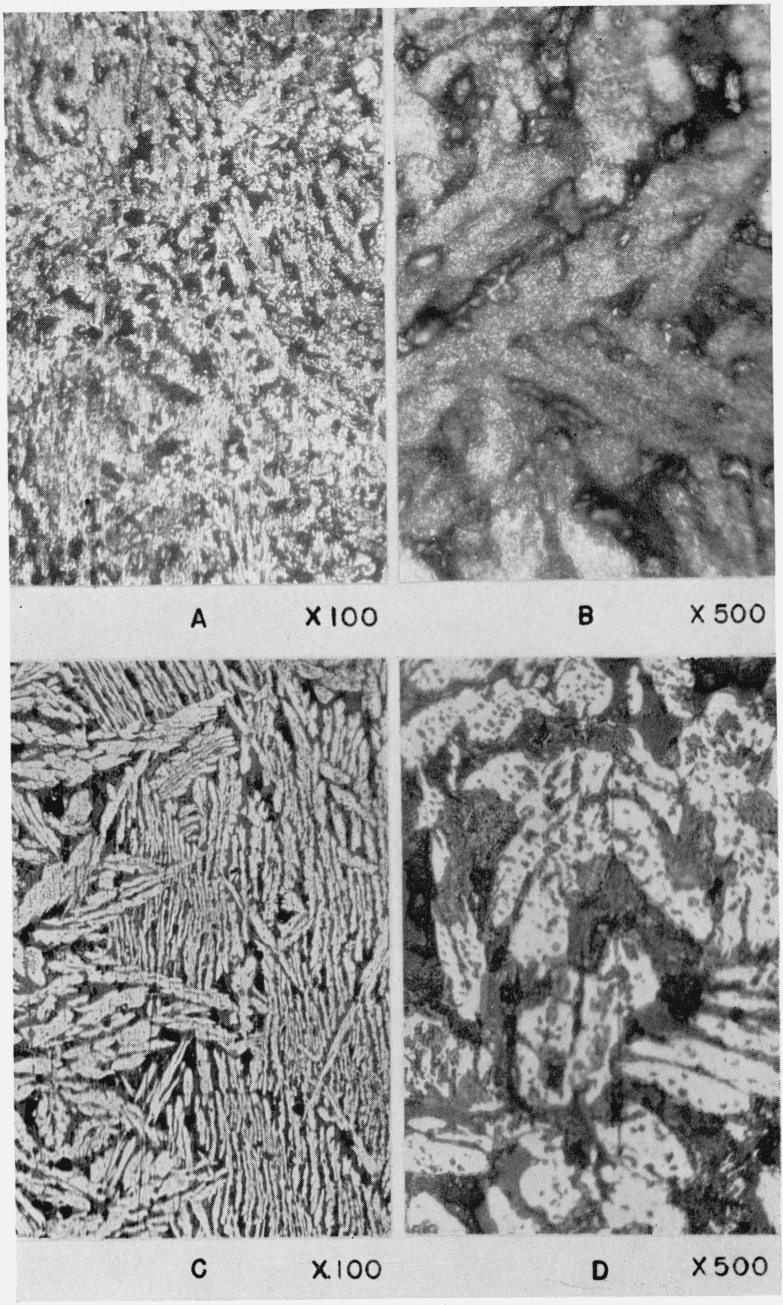

FIGURE 9.—*Aluminum bronze, 1 cycle per day, surface views, Severn River water,* $\times 4$.

60,000 lb/in.^{2}, 16 days.

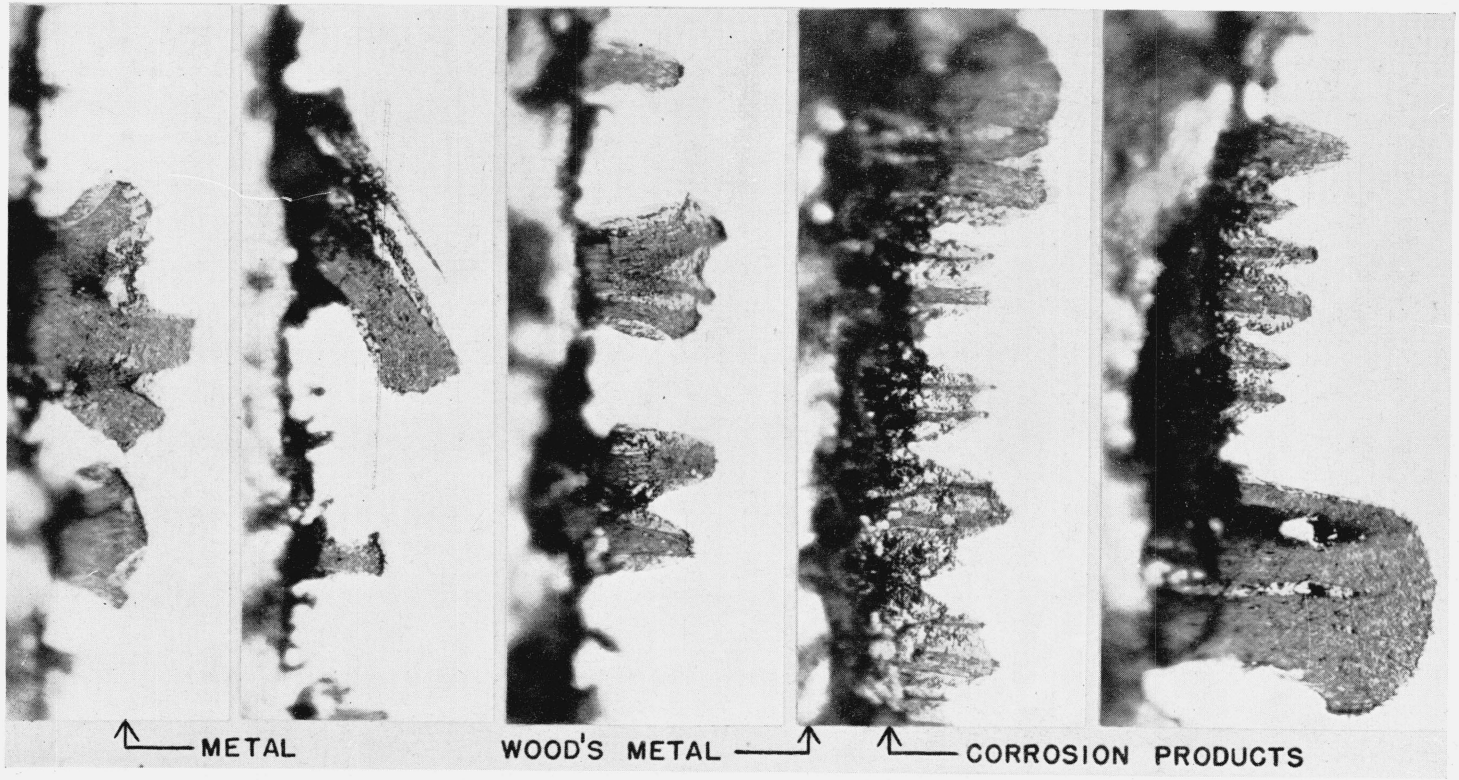

FIGURE 10.—*Aluminum bronze, 1 cycle per day, longitudinal sections, Severn River water, unetched,* $\times 1000$.

60,000 lb/in.^{2}, 16 days.

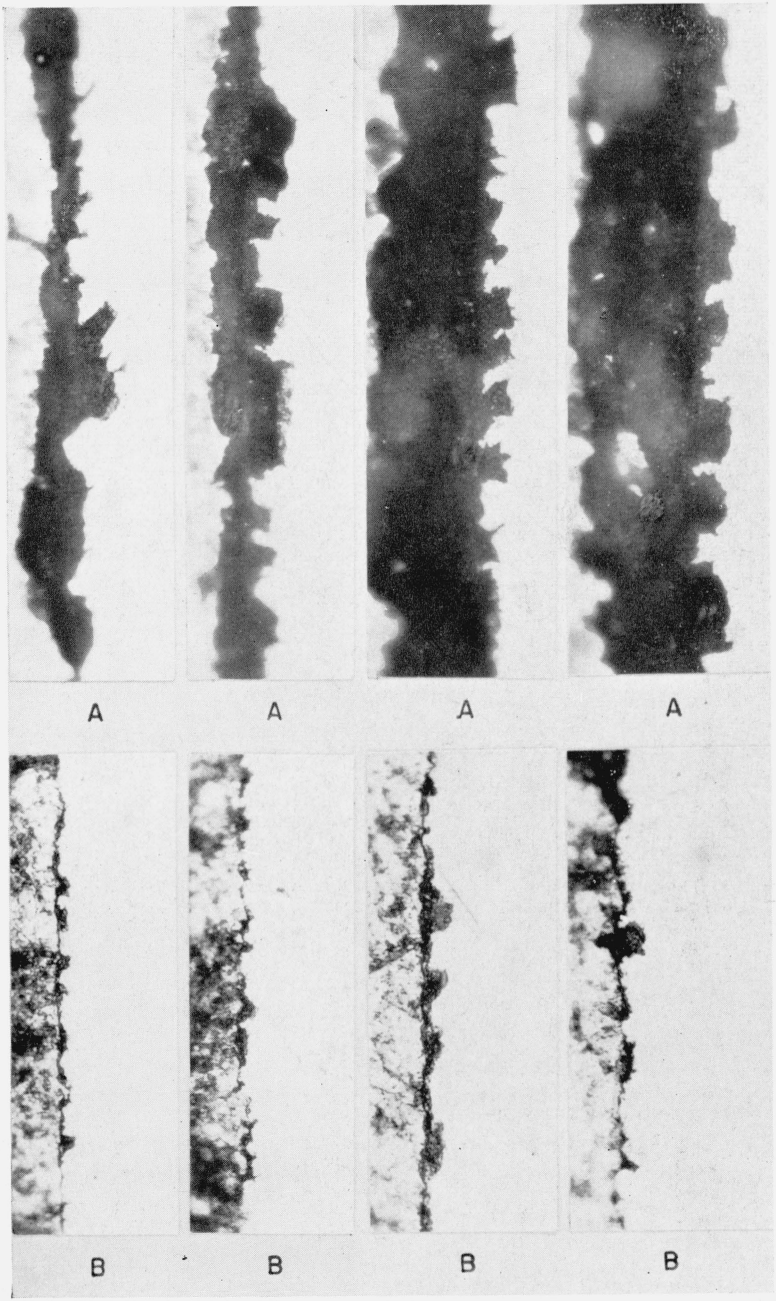

FIGURE 11.—*Aluminum bronze, stressless corrosion, longitudinal sections, well water* $\times 1000$.

A, 66 days.
B, 88 days.

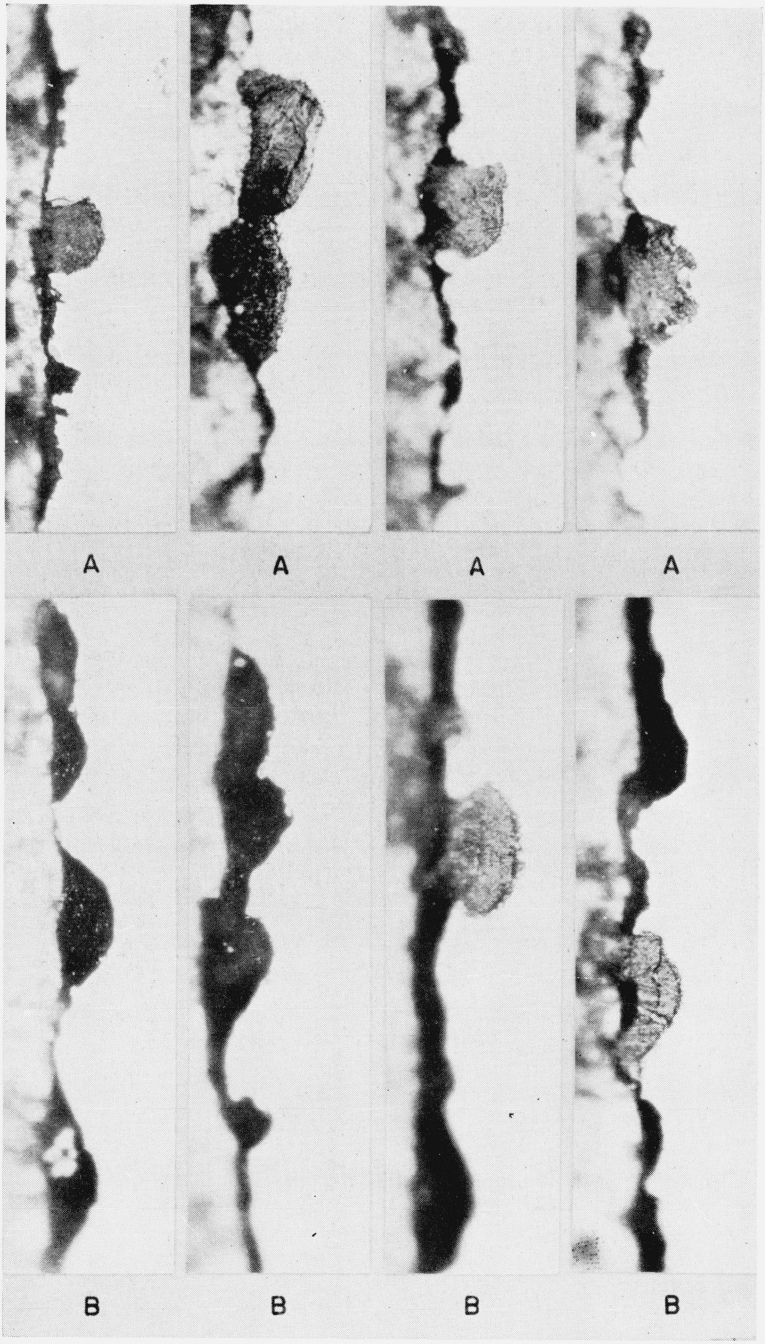

FIGURE 12.—*Aluminum bronze, stressless corrosion, longitudinal sections, well water, ×1000.*

A, 640 days.
B, 1,021 days.

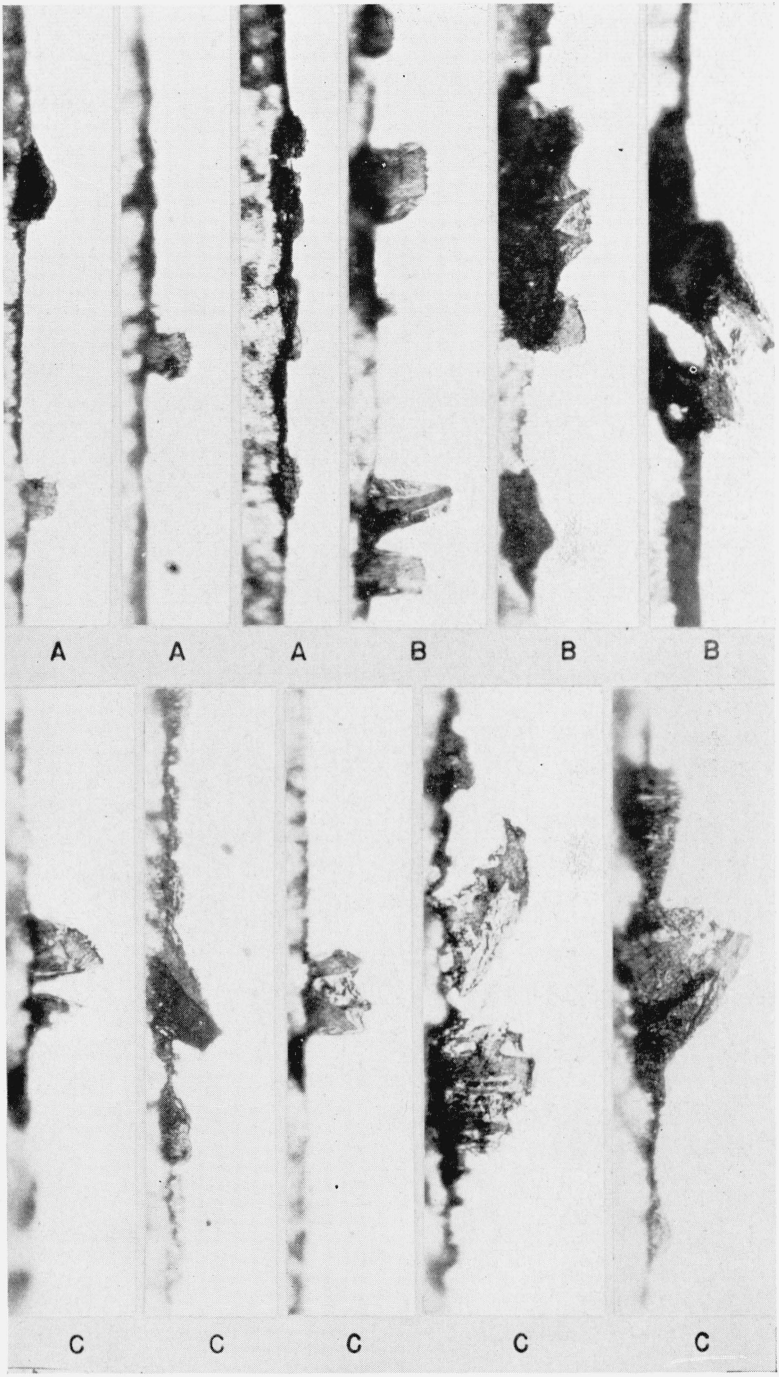

FIGURE 13.—*Aluminum bronze, 1,450 cycles per minute, longitudinal sections, well water, ×1000.*

A, 30,000 lb/in.², 1.8 days.
B, 25,000 lb/in.², 6 days.
C, 20,000 lb/in.², 11 days.

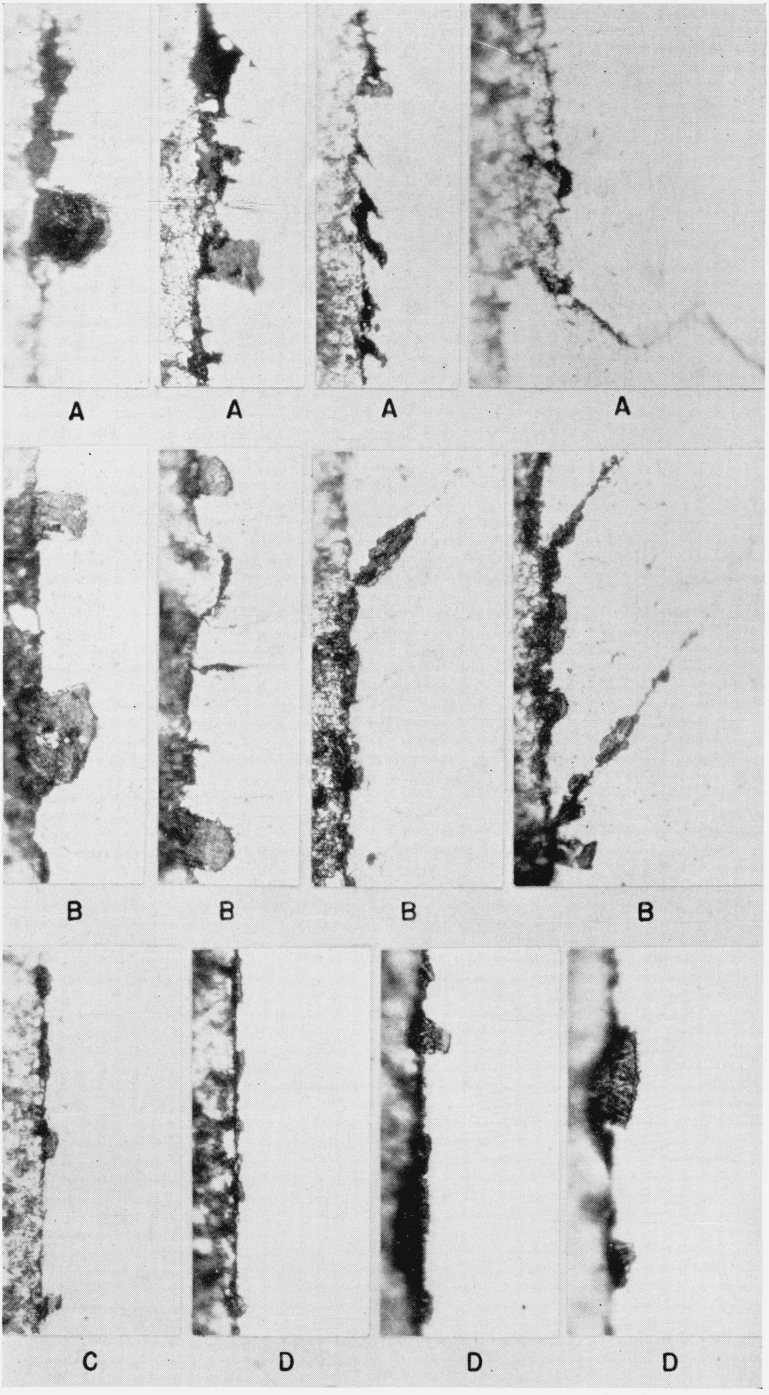

FIGURE 14.—*Aluminum bronze, longitudinal sections, well water, ×1000.*

A, 10,000 cycles per minute, 30,000 lb/in.^{2}, 0.3 day.
B, 500 cycles per minute, 60,000 lb/in.^{2}, 0.06 day.
C, 500 cycles per minute, 40,000 lb/in.^{2}, 0.7 day.
D, 500 cycles per minute, 30,000 lb/in.^{2}, 4.5 days.

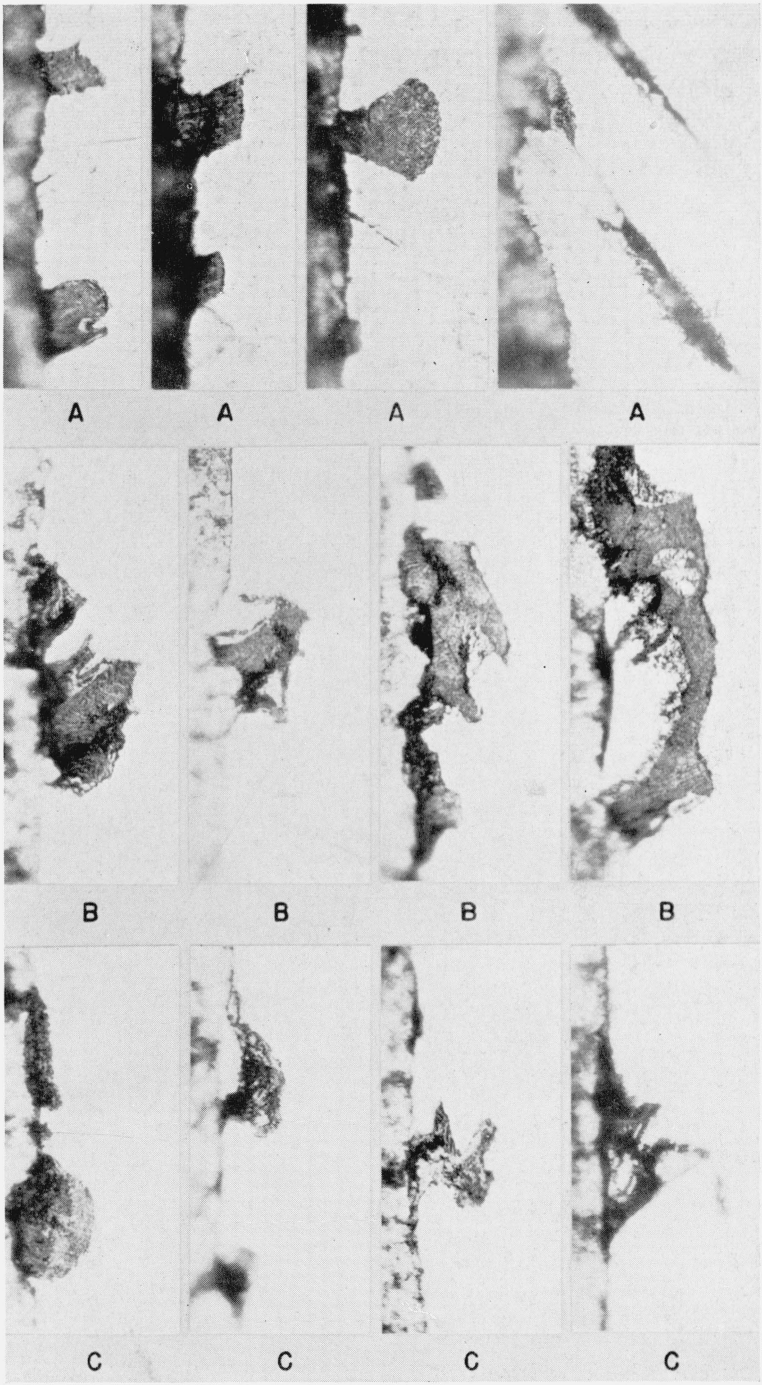

FIGURE 15.—*Aluminum bronze, 50 cycles per minute, longitudinal sections, well water, ×1000.*

A, 50,000 lb/in.², 1.1 days.
B, 35,000 lb/in.², 6.7 days.
C, 20,000 lb/in.², 52 days.

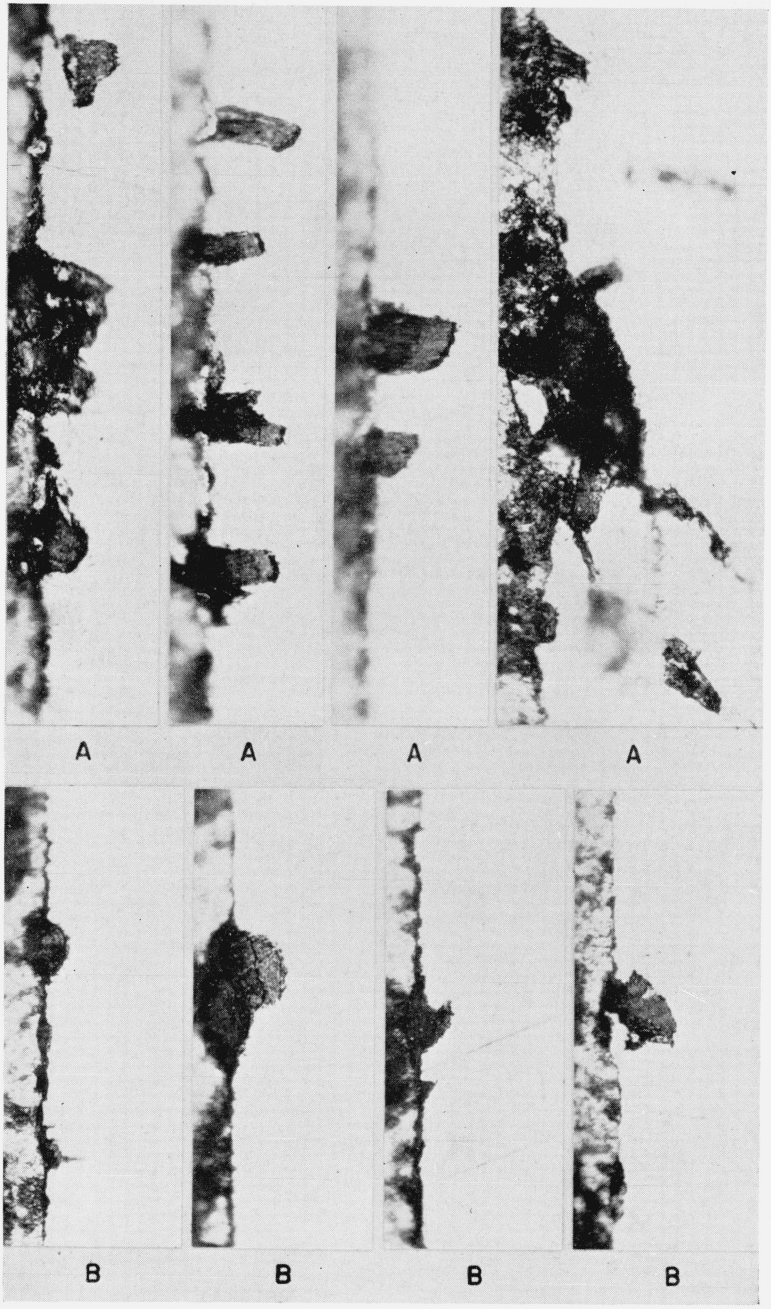

FIGURE 16.—*Aluminum bronze, 10 cycles per minute, longitudinal sections, well water, ×1000.*

A, 40,000 lb/in.^{2}, 13 days.
B, 30,000 lb/in.^{2}, 26 days.

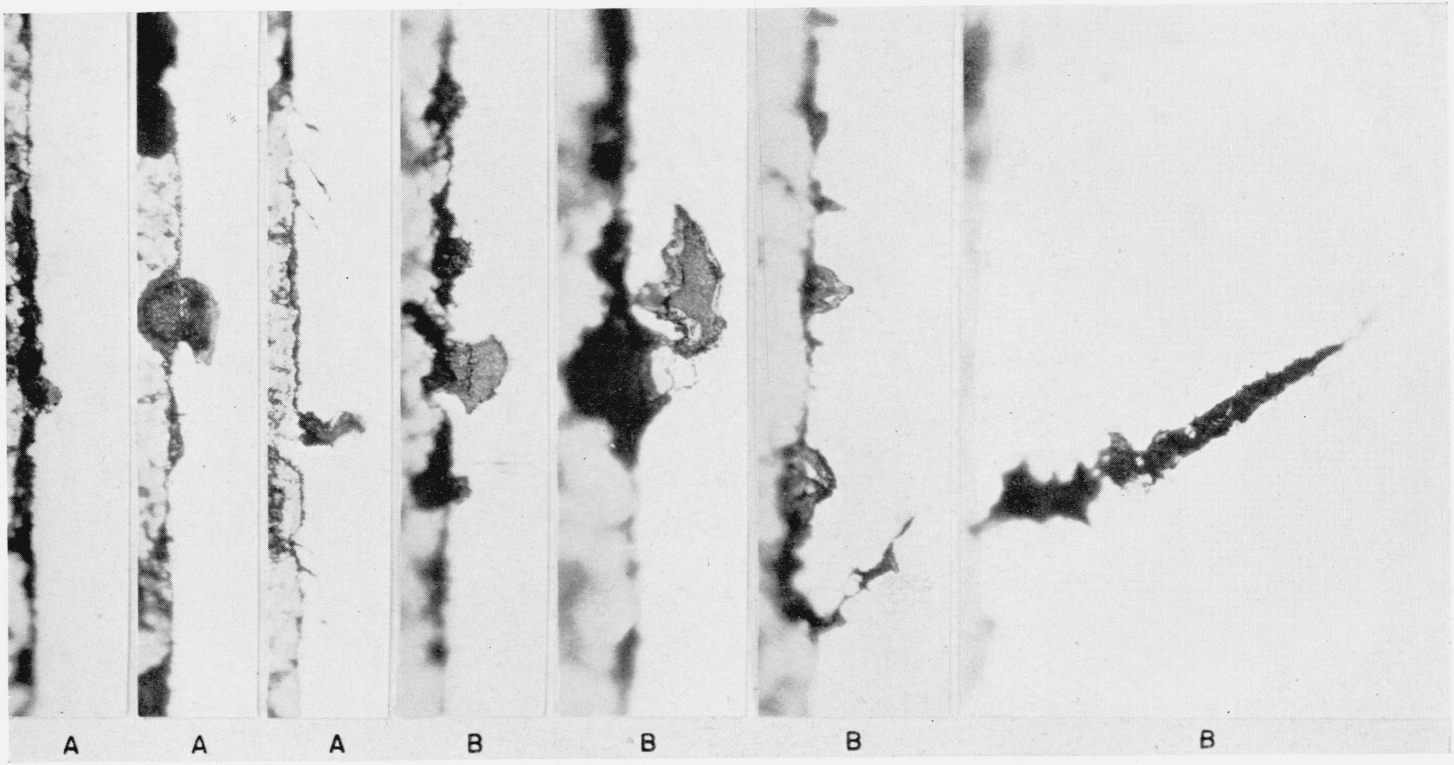

FIGURE 17.—*Aluminum bronze, 0.5 cycle per minute, longitudinal sections, well water,* $\times 1000$.

A, 60,000 lb/in.^{2}, 6 days.
B, 50,000 lb/in.^{2}, 13 days.

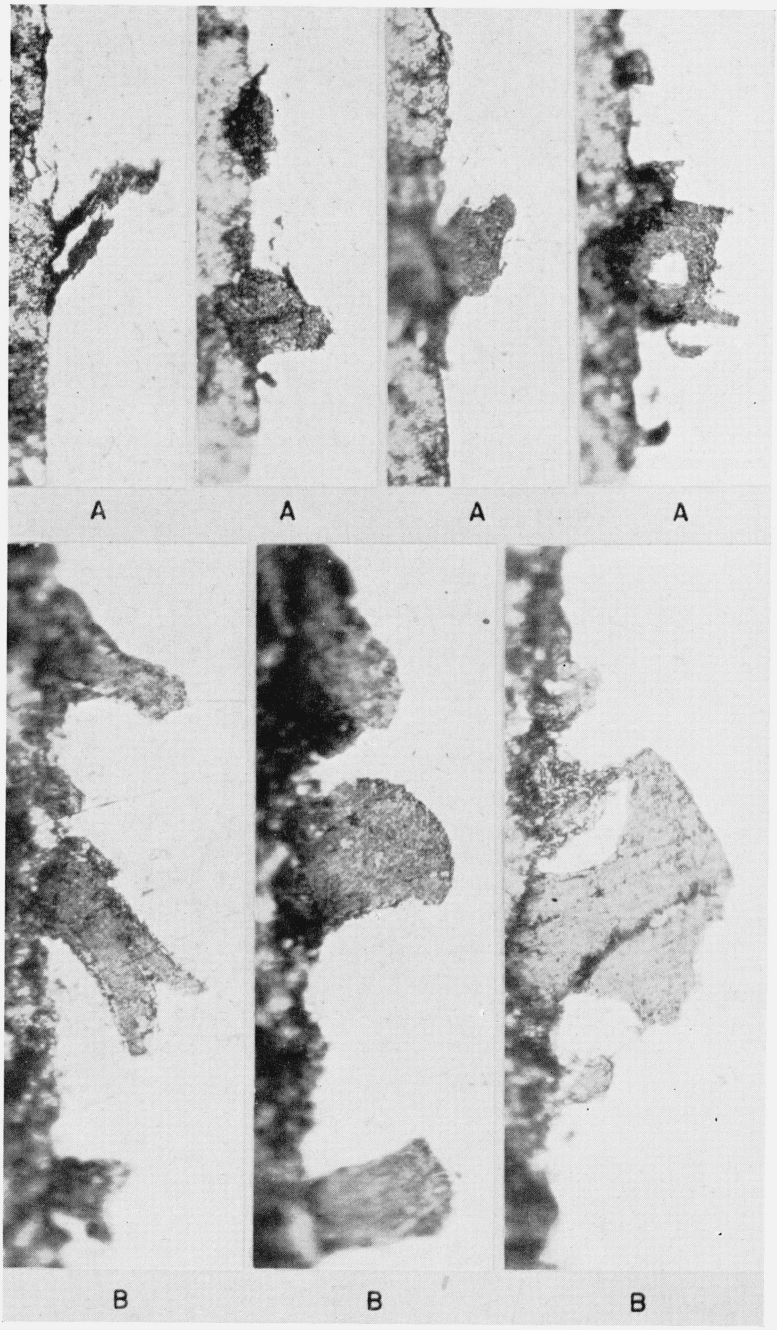

FIGURE 18.—*Aluminum bronze, 5 cycles per hour, longitudinal sections, well water, ×1000.*

A, 60,000 lb/in.², 15 days.
B, 50,000 lb/in.², 24 days.

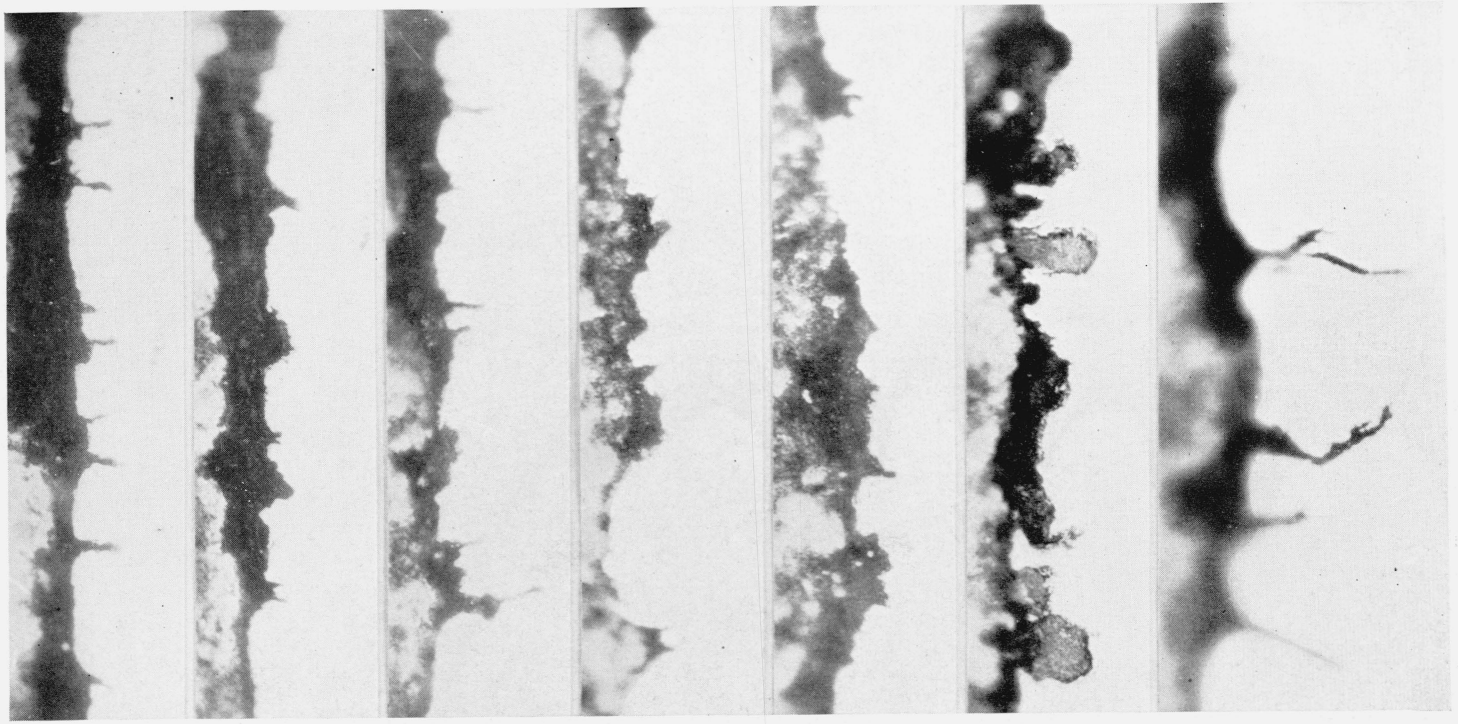

FIGURE 19.—*Aluminum bronze, 5 cycles per hour, longitudinal sections, well water, ×1000, 30,000 lb/in.², 339 days.*

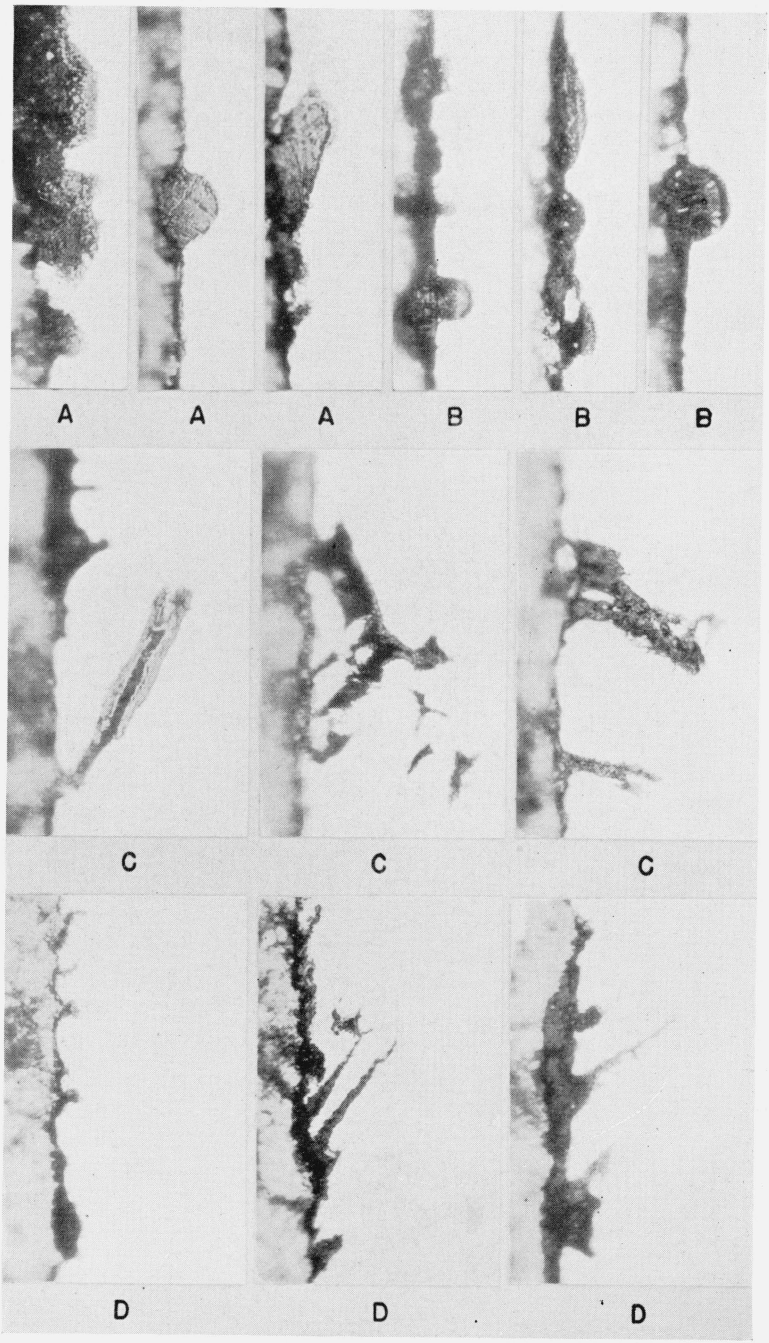

FIGURE 20.—*Aluminum bronze, 1 cycle per hour, longitudinal sections, well water, ×1000.*

A, 60,000 lb/in.^{2}, 20 days.
B, 40,000 lb/in.^{2}, 73 days.
C, 40,000 lb/in.^{2}, 149 days.
D, 35,000 lb/in.^{2}, 374 days.

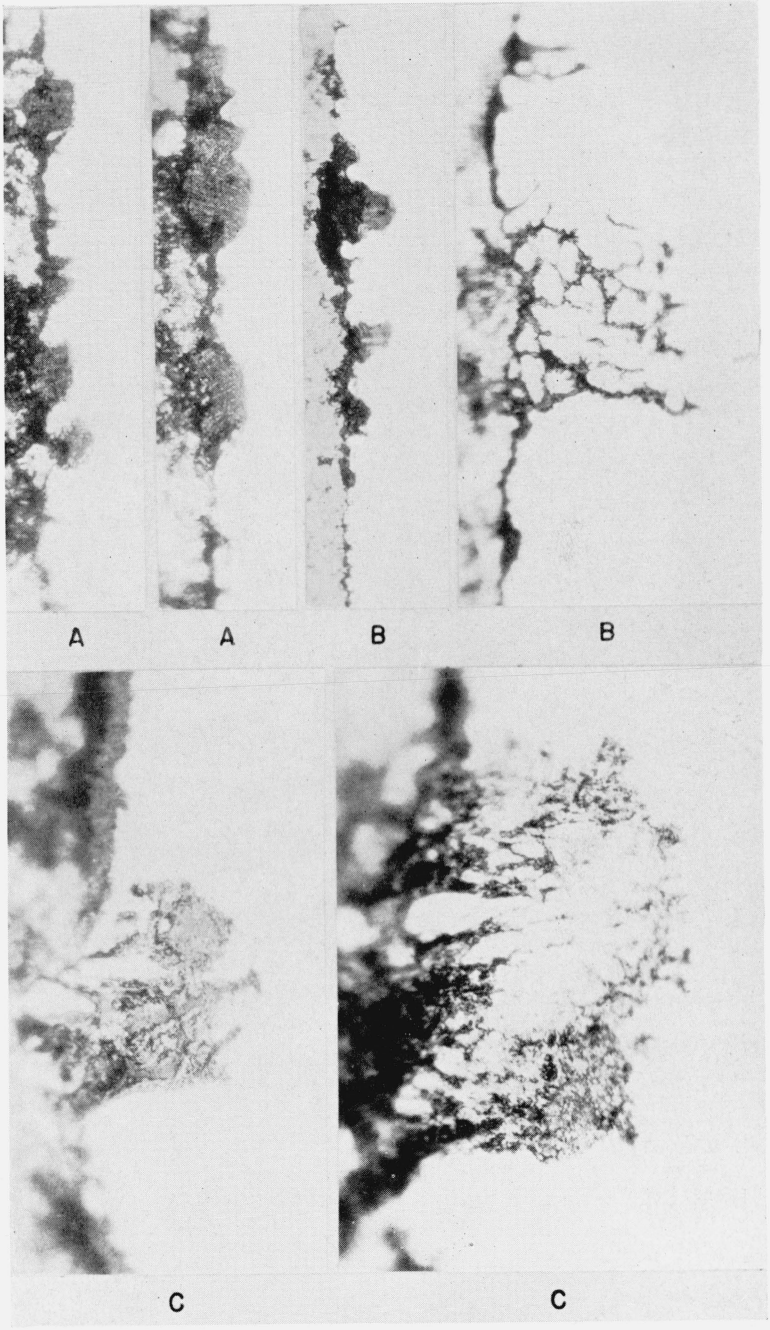

FIGURE 21.—*Aluminum bronze, 1 cycle per day, longitudinal sections, well water, ×1000.*

A, 60,000 lb/in.^{2}, 28 days.
B, 40,000 lb/in.^{2}, 151 days.
C, 40,000 lb/in.^{2}, 240 days.

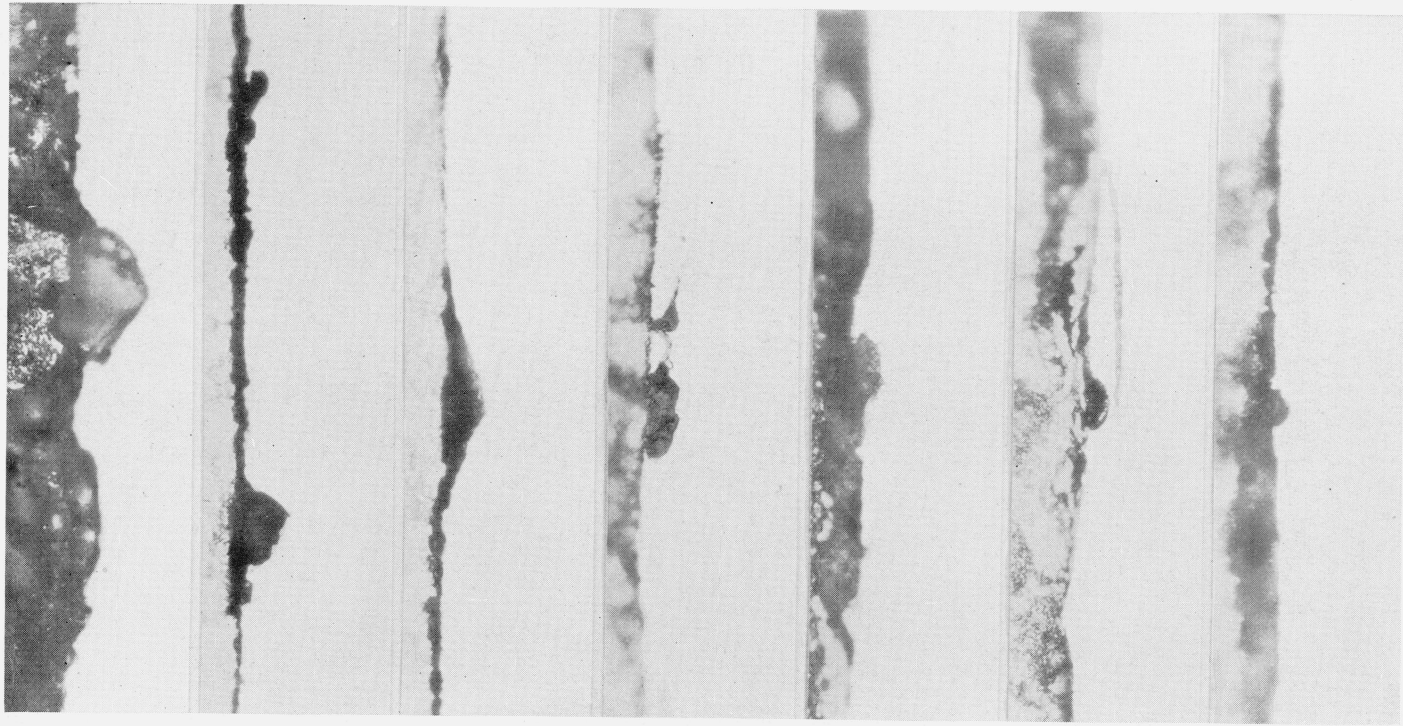

FIGURE 22.—*Monel metal, stressless corrosion, longitudinal sections, well water, ×1000. 122 days.*

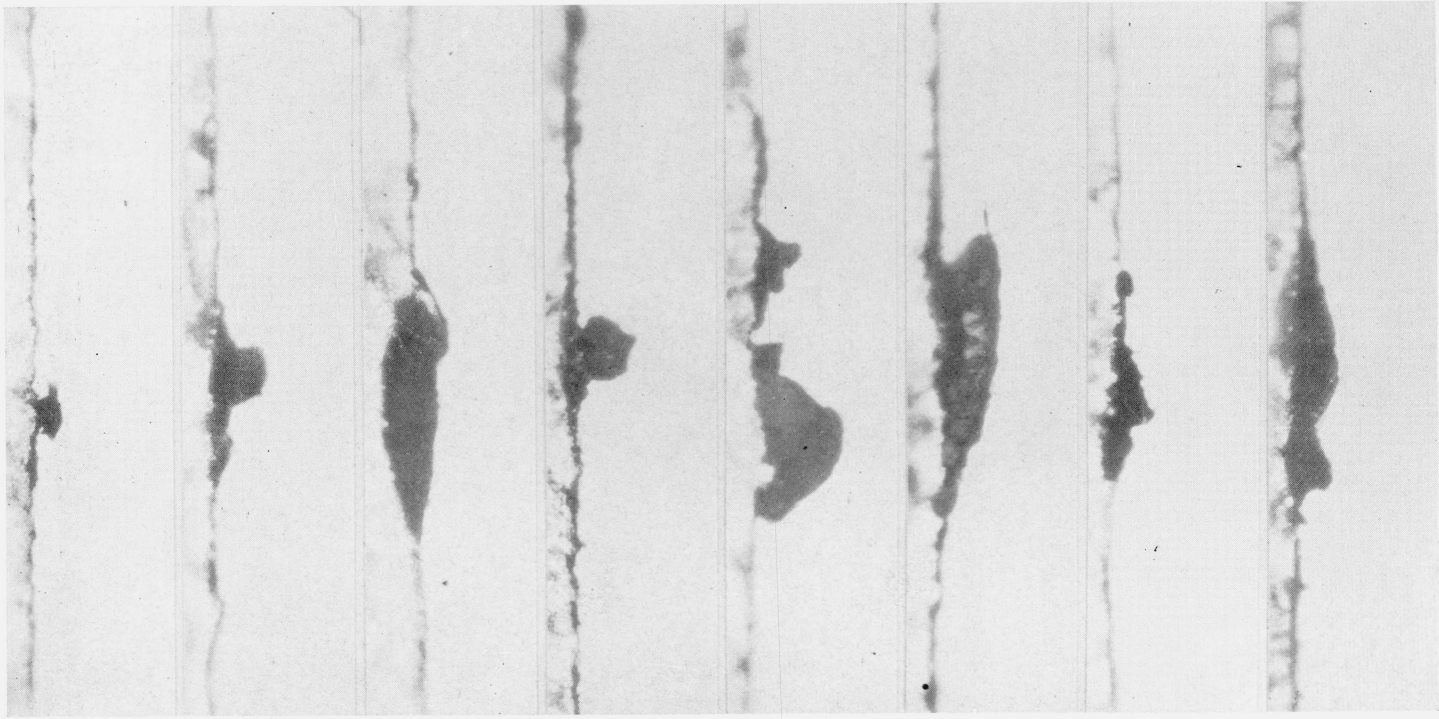

FIGURE 23.—*Monel metal, stressless corrosion, longitudinal sections, well water, ×1000. 157 days.*

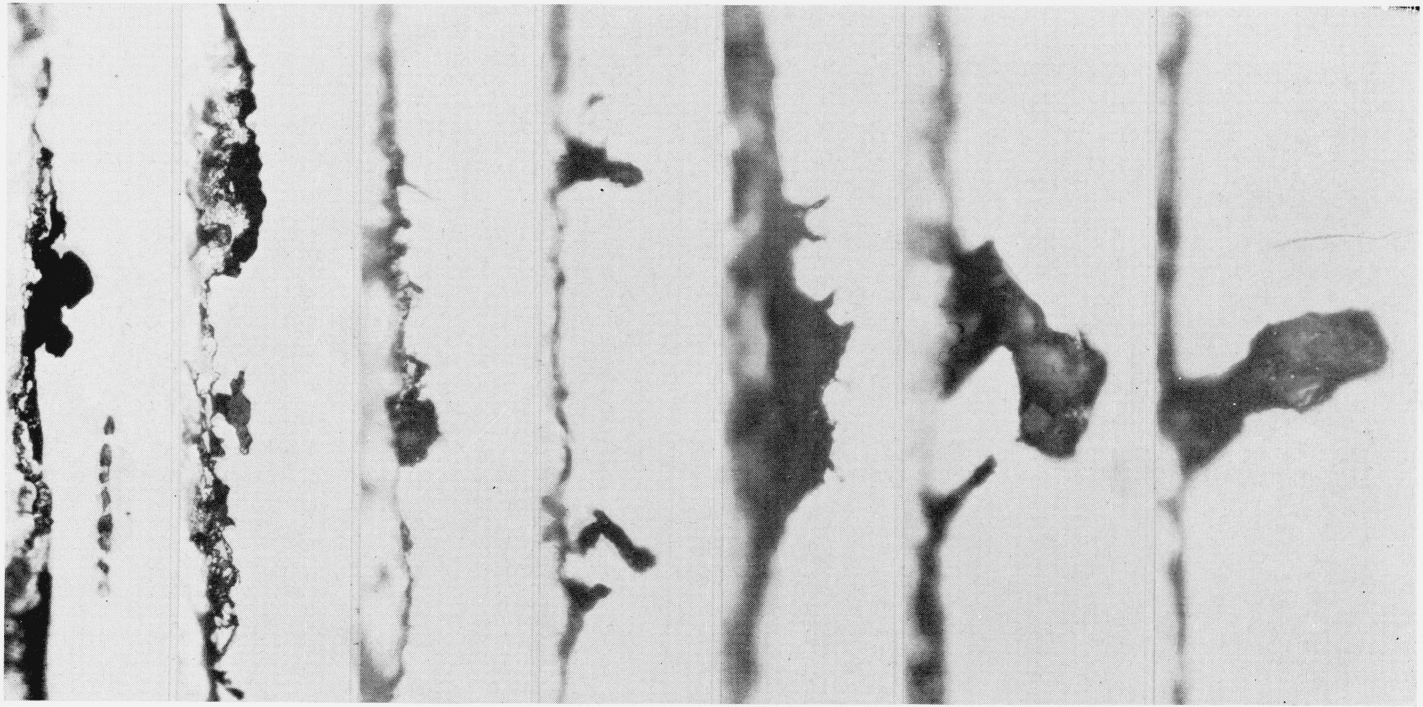

FIGURE 24.—*Monel metal, stressless corrosion, longitudinal sections, well water, ×1000. 170 days.*

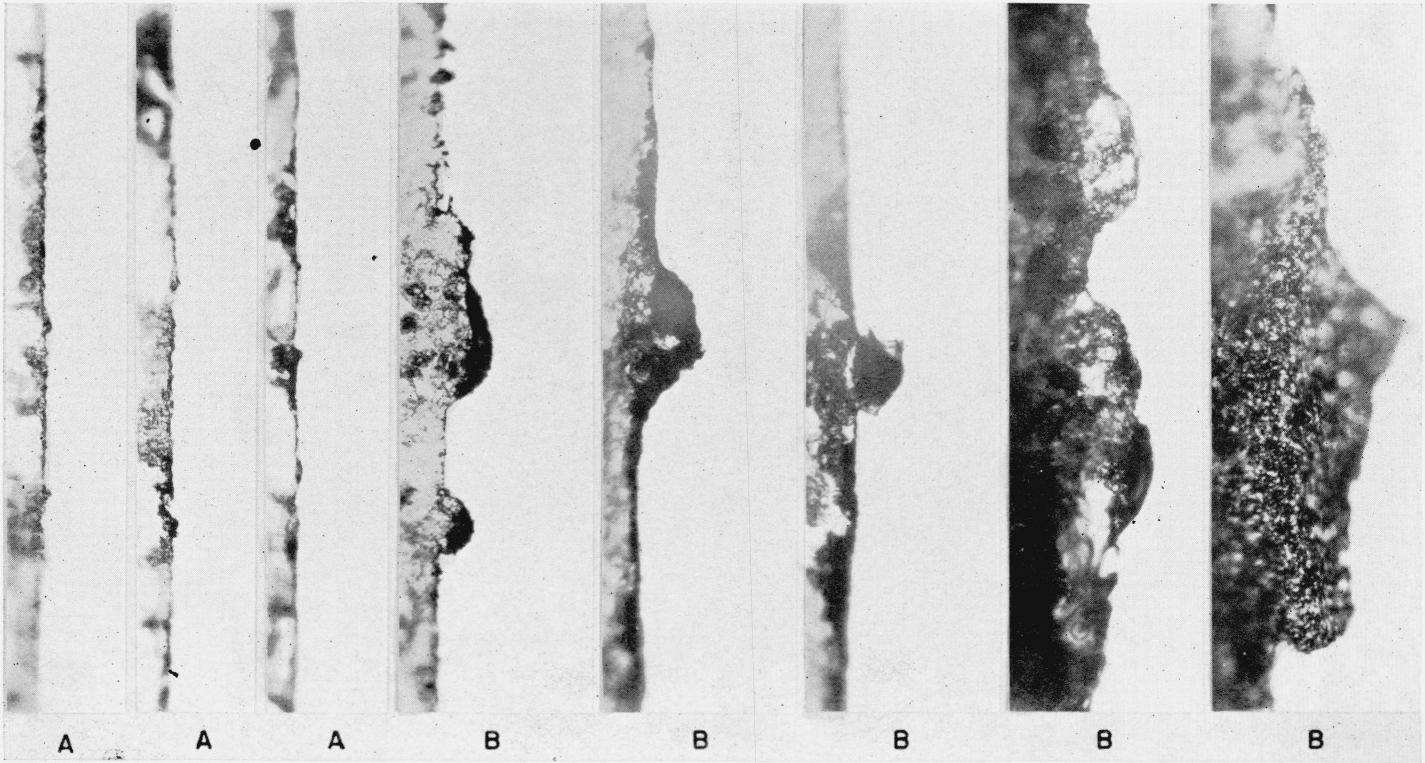

FIGURE 25.—*Monel metal, 1,450 cycles per minute, longitudinal sections, well water,* $\times 1000$.

A, 30,000 lb/in.^{2}, 10 days.
B, 10,000 lb/in.^{2}, 331 days.

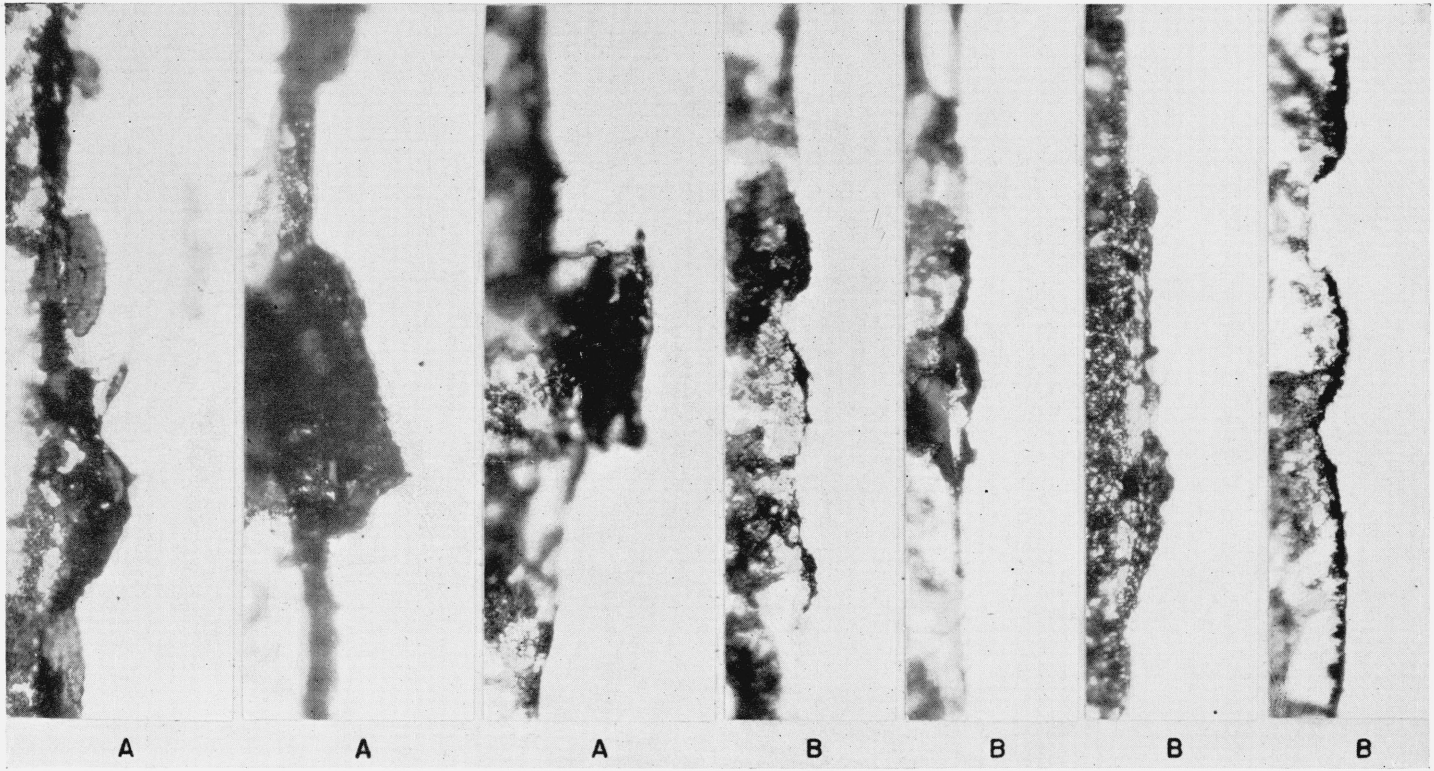

FIGURE 26.—*Monel metal, 5 cycles per hour, longitudinal sections, well water,* $\times 1000$.

A, 45,000 lb/in.^{2}, 123 days.
B, 40,000 lb/in.^{2}, 148 days.